CHAPTER

3

Climate change and melting glaciers

Maria Shahgedanova

Department of Geography and Environmental Sciences, University of Reading, Reading, United Kingdom

OUTLINE

1 Introduction

About 10% of the Earth's land surface or 15×10^6 km^2 is at present covered by glacier ice including ice sheets of Antarctica and Greenland, ice caps, and glaciers. About 91% and 8% of glacial ice is contained in the Antarctic and Greenland ice sheets, respectively. Ice caps, defined as bodies of ice with area of less than 50,000 km^2 and covering the underlying land completely, occur primarily in the polar and subpolar regions, for example, in the Canadian and Russian Arctic, Svalbard, and Iceland. Glaciers, which are often referred to as "small glaciers" irrespective of their size to distinguish them from ice sheets and ice caps, are located in polar and subpolar regions and in the mountains and span the whole range of elevations. In the polar and subpolar regions, they terminate in the ocean (tidewater glaciers) and in the High Mountain Asia (HMA) and in the Andes, descend from over 7000 m above sea level

https://doi.org/10.1016/B978-0-12-822373-4.00007-0

(a.s.l.). Estimates of the total area of glaciers and ice caps (including those in Greenland and Antarctica, but excluding the ice sheets) vary between 680×10^3 km^2 and 785×10^3 km^2 (Radić and Hock, 2010). Total glacier volume, based on the total area of 741×10^3 km^2, is estimated as $(241 \pm 29) \times 10^3$ km^3 (Radić and Hock, 2010). Farinotti et al. (2019) provides a lower estimate of $(158 \pm 41) \times 10^3$ km^3 which is equivalent to 0.32 ± 0.08 m of global mean sea level (GMSL) change.

About 69% of the world's fresh water is stored as ice. Glacial melt (including ice sheets and small glaciers) is responsible for about 50% of the observed sea level rise (Church et al., 2011; Oppenheimer et al., 2019). Glaciers deliver a range of ecosystem services (Huss et al., 2017). They are important sources of water (Viviroli and Weingartner, 2004; Viviroli et al., 2020) and in regions, where mountains are surrounded by arid plains, such as Central Asia and the Andes, glacial meltwater sustains irrigation without which sufficient food production may be impossible (Kaser et al., 2010). Healthy glaciers prevent the formation and expansion of glacier lakes and such hazards as glacier lake outburst floods (GLOF), mudflows, and landslides (Haeberli and Whiteman, 2015). It is estimated that in 2010, almost 10% (671 million people) of the global population lived in high mountain regions at a distance of less than 100 km from mountain glaciers and this population is expected to grow to 736–844 million (Hock et al., 2019). Those living in the mountains and residing further downstream depend on the ecosystem services provided by glaciers. Last but not least, glaciers have a high aesthetic value and represent some of the most spectacular landscapes in the world.

Glacial ice, in all its forms, is extremely vulnerable to climatic warming because its very existence depends on subzero temperatures. In the Arctic, summer temperatures, relevant to glacier melt, increased by 0.5–1.0°C in 2000–09 in comparison with 1960–2009 (Serreze and Barry, 2011). There is evidence that in the mountains, especially in the lower latitudes, climate is warming at a higher rate than on the plains (Pepin et al., 2015). It is not surprising that shrinking ice caps and glaciers have become symbols of the adverse effects of climate change.

In this chapter, the observed changes in the state of glaciers and ice sheets are reviewed together with factors initiating and controlling these changes. Indicators of glacier change and methods of assessments are discussed. The contribution of ice sheets and glaciers to sea level change is addressed.

2 Mass balance of glaciers and ice sheets

The state of glaciers, ice caps, and ice sheets depends on their mass balance (budget) defined as a difference between mass gain and mass loss in a given time period expressed either in metres of water equivalent (m w.e.) or in units of mass per year (Cuffey and Paterson, 2010). Glaciers which receive more (less) mass than they lose, have positive (negative) mass balance. They advance and thicken (retreat and thin). Glaciers, gaining and losing approximately the same mass have zero mass balance and if this persists over time, they are said to be in a state of equilibrium and their termini neither advance nor retreat. Mass gain occurs by accumulation of snow from direct precipitation, windblown snow, or avalanches on glacier surface. Net accumulation occurs in the upper part of glaciers, in the accumulation zone, where accumulated snow is transformed into firn and then ice which over years flows downslope. For glaciers terminating on land, mass loss (ablation) is dominated by melt in the lower

part of glaciers but can also occur via sublimation while basal melting is usually a smaller term. For temperate glaciers, liquid precipitation and meltwater are considered as runoff. Sublimation is particularly important for tropical glaciers. For example, at Kilimanjaro, ice loss occurs almost entirely through sublimation (Kaser et al., 2004; Mölg et al., 2008).

Difference between accumulation and ablation on the surface forms surface mass balance (SMB). The elevation, at which net accumulation equals net ablation is known as the equilibrium line altitude (ELA). If a glacier is receding, its ELA progressively moves up, making the accumulation area ratio (AAR) smaller. In colder areas (either geographical or at higher elevations), liquid precipitation and meltwater percolate into ice and refreeze, resulting in internal accumulation which, together with SMB, forms climatic mass balance. Confusingly, in ice sheet studies, climatic mass balance can be referred to as SMB to distinguish it from ice discharge (van den Broeke et al., 2017).

For marine-terminating glaciers (as well as for those terminating in lakes) and ice sheets, front calving and melting underneath floating ice shelves are important components of ice loss and they are often aggregated as ice discharge or dynamic ice loss (D) across the grounding line, a zone of transition from grounded ice to freely floating ice (e.g., ice sheet to ice shelf). Knowledge of its position is important because ocean warming around the grounding line can cause rapid melt, increase in ice velocity, and ice discharge to the ocean (Rignot, 1996). If SMB equals D, ice mass is in balance providing that basal melt is negligible (Cuffey and Paterson, 2010).

Mass balance is controlled primarily, but not exclusively, by air temperature of the ablation season and by precipitation. The length of the ablation season varies from a few weeks in the polar regions to all year in the tropics. Increasing air temperature can lead to both more intense melt and an extension of the melt season increasing mass loss. Thus, the progressively more negative mass balance of Glacier de Sarennes in the French Alps during the 1949–2007 period was caused by summer warming with the lengthening of the ablation season and higher ablation rates explaining 65% and 35% of the increase in glacier melt, respectively (Thibert et al., 2013). Precipitation during the accumulation season controls mass gain. For example, a decline in precipitation in the 1970–80s in Central Asia significantly contributed to glacier mass loss in the Tien Shan (Shahgedanova et al., 2018). The occurrence of solid precipitation during the ablation season is also important because it interrupts and reduces ablation by changing the albedo (reflectivity) of the glacier surface. For this reason, the high-elevation glaciers of Kilimanjaro are more sensitive to changes in precipitation than temperature (Mölg et al., 2008). Atmospheric humidity controls sublimation which is particularly important for tropical glaciers (Vuille et al., 2008; Rabatel et al., 2013). Cloudiness controls both incoming long-wave and short-wave radiation. Melt at the highest elevations in Greenland is caused by the long-wave radiation emitted by clouds (van den Broeke et al., 2017). Short-wave radiation is a particularly important source of energy for melt in combination with surface albedo. The transition from fresh snow to wet, aged snow, and ice and the presence of light absorbing impurities (LAI) on the glacier surface strongly influence melt particularly when solar radiation values are high. Changes in sea surface temperature (SST) and heat supplied to glacier tongues by the ocean affect mass loss from marine-terminating glaciers.

The response of glaciers to climatic perturbations is not uniform because glaciers have different SMB sensitivities to climatic forcing and different response times. Sensitivity is the change in mass balance per unit change in a climatic variable such as air temperature or

precipitation. Sensitivity depends on climate (as a rule, maritime glaciers have higher sensitivity than continental glaciers because they have high mass turnover), slope, and morphology of glacier. The response time is the time which is required for a glacier to adjust to a change in mass balance. Small cirque glaciers react to changes in climate and mass balance almost without delay; short and steep glaciers reach equilibrium in a few years while larger valley glaciers have a response time of several decades (Haeberli, 1995).

Mass balance is used to calculate glacier and ice sheet contributions to GMSL change. However, change in mass and contribution to GMSL are not identical. Changes in floating ice shelves do not cause any significant changes in GMSL directly although there is a negligible effect because of changes in the salinity of ocean water. However, ice shelves buttress marine ice sheets and their demise can cause marine ice-sheet instability resulting in a discharge of land ice into the ocean. Therefore, for ice sheets and marine-terminating glaciers, change in mass balance and contribution to GMSL are different because they contain floating ice and because of the effects of a migrating grounding line. A more detailed explanation is provided by Bamber et al. (2018). There is also a difference in the case of glaciers in landlocked (endorheic) basins, for example, in the Pamir and Tien Shan in Central Asia, because water, which they lose, may never directly reach the ocean, contributing to GMSL only indirectly through land hydrology processes (Brun et al., 2017). Meltwater can be withdrawn for human use or stored in glacial lakes (Haeberli and Linsbauer, 2013). For example, in Patagonia, terrestrial storage in the lakes of the Northern Patagonian Icefield is as high as 10% of its glacier melt contribution to sea level rise (Loriaux and Casassa, 2013).

3 Observing glacier change

3.1 Measuring mass balance

Glacier mass balance is measured either by glaciological (stake) or geodetic methods (Cogley, 2009; Zemp et al., 2009, 2015). Both annual mass balance rates and cumulative mass balance, showing glacier mass in a given time period relative to an earlier one, are used. The glaciological method involves establishing a grid of ablation stakes across a glacier, measuring accumulation and ablation with reference to the stakes several times per year, and interpolating measurements across the glacier surface. These measurements are accompanied by snow density measurements (to calculate water equivalent) and supported by meteorological observations. The surveys are time-consuming, physically demanding, and occasionally dangerous. They have limited coverage but provide the longest mass balance series dating back to the late 19th (the Rhone glacier)—early 20th (the Silvretta glacier) centuries (Zemp et al., 2009). Glaciological mass balance measurements are coordinated by the World Glacier Monitoring Service (WGMS). In the 1946–2005 period, results were available from 228 glaciers around the world but only 12 provided time series dating back to 1960 or earlier (Zemp et al., 2009). For climate change assessments, ongoing mass balance series with over 30 observation years are used from the so-called reference or benchmark glaciers. Fig. 1 shows two of these glaciers, Tuyuksu in the Tien Shan and Djankuat in the Caucasus. Fig. 2 shows cumulative mass balance of the Tuyuksu glacier which has the longest uninterrupted data series in Central Asia.

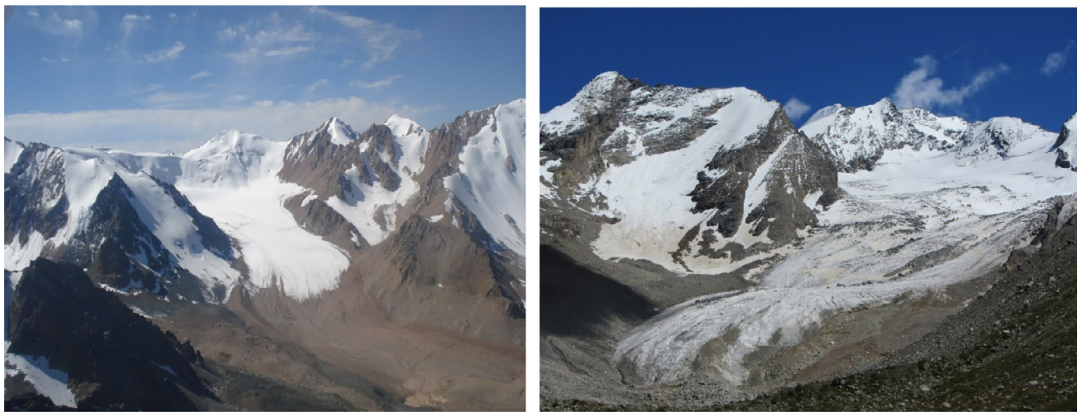

FIG. 1 The WGMS reference glaciers: Tuyuksu in the Tien Shan (left-hand panel) and Djankuat in the Caucasus (right-hand panel).

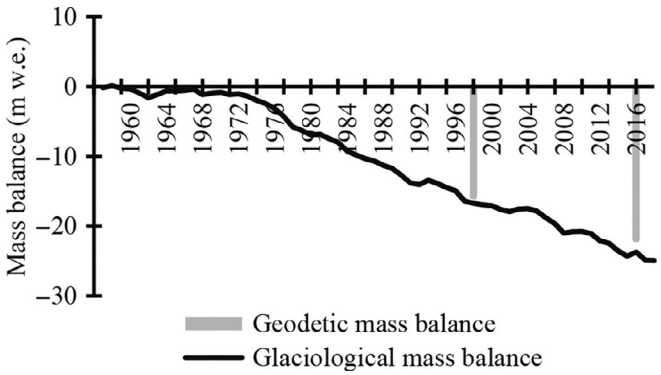

FIG. 2 Cumulative mass balance of the Tuyuksu glacier, Tien Shan, measured using the glaciological method and geodetic mass balance for the 1958–98 and 1958–2016 periods (Kapitsa et al., 2020). Using both methods helps to verify data quality: A close match between the two types of measurements confirms data reliability. Note that cumulative mass balance has been persistently negative since the 1970s indicating that Tuyuksu is losing mass.

The geodetic method is based on repeated measurements of glacier surface elevation using consecutive digital elevation models (DEM) developed from field surveys, aerial, and spaceborne data (Cogley, 2009; Marzeion et al., 2017). Satellite radar (ERS-1, ENVISat, CryoSat 2) and laser (ICESat) altimetry is used to measure changing surface elevation of ice sheets, ice caps and, in the case of ICESat, larger glaciers (Bamber et al., 2018). The Shuttle Radar Topography Mission (SRTM) provides elevation data collected between 60°N and 54°S in 2000. Photogrammetric methods using repeat airborne and optical satellite imagery such as ASTER (e.g., Brun et al., 2017) and submetre Pléiades (e.g., Berthier et al., 2014; Kutuzov et al., 2019; Kapitsa et al., 2020) enable development of higher-resolution DEMs from spaceborne data for smaller mountain glaciers worldwide. Fig. 3 shows changes in the surface elevation of the Tuyuksu glacier between 1958 and 2016 derived from a ground-based geodetic survey

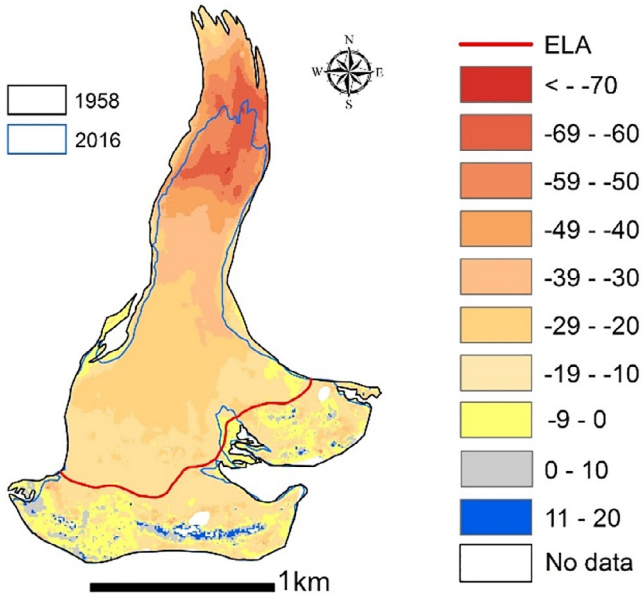

FIG. 3 Changes in the surface elevation of the Tuyuksu glacier between 1958 and 2016, derived from a ground-based geodetic survey and the Pléiades imagery (Kapitsa et al., 2020). These data were used to derive the geodetic mass balance of the Tuyuksu glacier (Fig. 2). Note that at the lower part of the glacier, surface lowering exceeded 60 m and about 23% of the glacier area has been lost.

and the Pléiades imagery. The USA declassified spy Corona and Hexagon imagery, particularly plentiful over the territory of the former Soviet Union, enables development of historical DEM from the 1970s (e.g., Pieczonka and Bolch, 2015). Using these data, changes in glacier volume are measured and converted to mass balance using glacier-averaged density (Huss, 2013). Thus, the geodetic mass balance of the Tuyuksu glacier (Fig. 2) was derived from changes in surface elevation (Fig. 3). The geodetic method expands geographical coverage of mass balance measurements and extends them to inaccessible parts of glaciers. The use of spaceborne data enabled global assessments, particularly measurements of mass balance of ice caps and ice sheets, and this method is widely used in calculations of glacier contribution to sea level rise (Marzeion et al., 2017).

Gravimetric method of measuring changes in glacier mass at the global scale became available since the launch of the Gravity Recovery and Climate Experiment (GRACE) twin satellites in summer 2002 (Wahr et al., 2004). Changes in gravity are mainly caused by changes in the mass of surface water and, therefore, gravity anomalies provide information about its redistribution. GRACE has a coarse resolution of 300 km and is used predominantly to measure changes over ice sheets (Velicogna, 2009; Bamber et al., 2018) or ice caps and larger polar glaciers (Jacob et al., 2012; Box et al., 2018). Attempts were made to use GRACE to assess changes in mass of mountain glaciers (Jacob et al., 2012) but with limited success because the coarse resolution resulted in a very high uncertainty. Changes in regional hydrology, particularly water withdrawal for irrigation in Central Asia, affected the redistribution of mass and the quality of measurements.

All sources of data and methods are valuable and their complementary use enables validation of data sets, accuracy assessments, and inter-comparison of measurements leading to a wider coverage and an improved quality of observations. For example, the Pléiades Glacier Observatory was established by the WGMS in collaboration with the French Space Agency (CNES) to expand mass balance monitoring from individual benchmark glaciers to regional scale through the application of the high-resolution Pléiades satellite DEM validated with ground control data (see, e.g., Fig. 2 as well as Berthier et al., 2014; Kutuzov et al., 2019; Kapitsa et al., 2020) and to fill in gaps in observations (e.g., Barandun et al., 2018). Another example is the Ice Sheet Mass Balance Inter-comparison Exercise (IMBIE) project who combined assessments of changes in the mass balance of the Antarctic and Greenland Ice sheets derived from satellite altimetry, gravimetry, and the so-called mass balance input-output method, comparing modeled SMB with satellite-derived ice flow (D), to reduce uncertainty of these complex assessments and improve our understanding of glacier contribution to sea level change (The IMBIE Team, 2018, 2020).

3.2 Measuring changes in glacier length and area

Another way to assess glacier change is to measure changes in glacier length (position of glacier termini or front variations) or area. Glacier length data sets go back the furthest. This is because direct field observations of the position of glacier tongues were the earliest type of measurement to be taken and because it is relatively easy to map the past locations of glacier fronts on satellite images by identifying the Little Ice Age (LIA) moraines which usually mark the maximum extent of glaciers over the last millennium. There are numerous regional studies. For example, Stokes et al. (2006) mapped changes in glacier length in the Caucasus Mountains from their LIA extent at multiple intervals using Landsat and Corona imagery while Solomina et al. (2016a) used lichenometry to date terminal moraines and tree-ring climatic reconstructions to extend the record to the end of the 16th century. They attributed changes in glacier length to changes in temperature. Lichenomtery and radiocarbon dating of moraines were used to develop detailed chronologies of glacier fluctuations during the LIA in the tropical Andes (Rabatel et al., 2013). A global data set, containing over 470 lengths with the longest dating back to 1535, was developed by Leclercq et al. (2014). Selected records from this data set are shown in Fig. 4. Solomina et al. (2016b) developed a global data set detailing glacier length change over the last 2000 years. Several world-wide data sets were used in assessment of impacts of climate change on glaciers and to model glacier contribution to sea level rise (Oerlemans et al., 2007; Oerlemans, 2010; Leclercq et al., 2011). WGMS has a collection of glacier frontal variations containing about 40,000 observations of about 2000 glaciers extending back to the 16th century.

A global initiative Global Land Ice Monitoring from Space (GLIMS) was launched to monitor changes in glacier area worldwide using optical satellite imagery (Raup et al., 2007; Bhambri and Bolch, 2009; Kargel et al., 2014). A globally complete inventory of glacier outlines—the Randolph Glacier Inventory (RGI)—was produced (Pfeffer et al., 2014) and its latest version, released in 2017, includes 215,547 glaciers (RGI Consortium, 2017). Numerous regional studies report changes in glacier area from the 1980s using first Landsat and later ASTER imagery and extend assessments back in time by using aerial photography, Corona and Hexagon satellite imagery, and by mapping positions of glacial moraines using modern

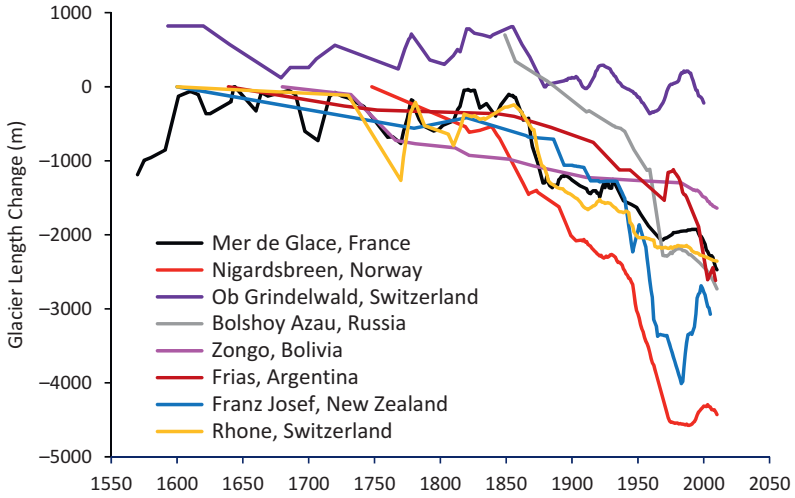

FIG. 4 Examples of the long-term records of glacier length change (m) from different parts of the world. *Data are from Leclercq, P.W., Oerlemans, J., Basagic, H.J., Bushueva, I., Cook, A.J., Le Bris, R., 2014. A data set of worldwide glacier length fluctuations. Cryosphere 8, 659–672. doi:10.5194/tc-8-659-2014.*

satellite images. For example, Kutuzov and Shahgedanova (2009) and Shahgedanova et al. (2012) used these multiple sources to quantify changes in glacier area at multiple time steps in the Tien Shan and in the Polar Urals, respectively. Repeat terrestrial photographs taken from the same vantage point, at the same time of year but years apart are used to assess changes in individual glaciers providing important historical perspective. Repeated images of the MGU glacier in the Polar Urals are shown in Fig. 5. Excellent archives of repeated photographs are available from the National Snow and Ice Data Center (NSIDC) and WGMS.

Assessments of changes in glacier area over multiple time steps are useful because they provide information about trends through time (i.e., acceleration of glacier wastage which can be attributed to changes in climate), elevational dependencies, and enable comparisons between regions and different types of glaciers. When making these comparisons, however, one should keep in mind that absolute changes in glacier length and area depend on length and area itself and relative changes produce a more coherent global pattern. Accurate glacier outlines improve calculations of geodetic mass balance, constrain spaceborne gravimetric measurements and provide input to various glaciological and hydrological models. Information about area change is important in assessments of glacial hazards: glacial lakes (and potential GLOF) develop following glacier retreat and knowledge about glacier area and its change helps to model the development of existing and formation of future glacier lakes (e.g., Kapitsa et al., 2017).

4 Observed changes in the state of ice sheets and glaciers

Since the end of the 19th century glaciers and ice caps have been thinning and retreating worldwide in response to climatic warming (with exception of a small number of regions) and this trend intensified in the second half of the 20th century. Recently, several estimates of

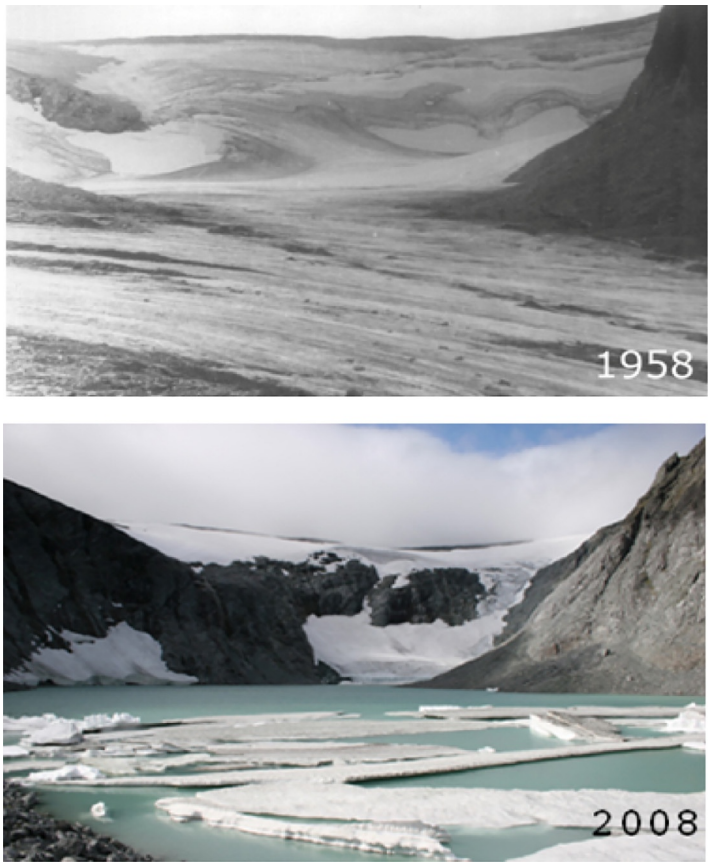

FIG. 5 Repeated ground-based photographs of the MGU glacier, Polar Urals. See Shahgedanova et al. (2012) for discussion of glacier change in this region. *Photo from 2008 is by G. Nosenko, Institute of Geography, Russian Academy of Science.*

global-scale glacier mass budget, based on different methods, were published (Church et al., 2011; Gardner et al., 2013; Bamber et al., 2018; Wouters et al., 2019; Zemp et al., 2019; IPCC, 2019). Both remote sensing, in situ measurements, and all indicators of glacier change confirm that there is a globally coherent pattern of negative mass budget and glacier recession (Zemp et al., 2015, 2019). Despite significant decadal and regional variations, the recent IPCC Special Report on the Ocean and Cryosphere in a Changing Climate (SROCC) stated that there is very high confidence in this conclusion (Hock et al., 2019).

Reliable assessments of changes in mass of the Antarctic ice sheet (AIS) and Greenland ice sheet (GrIS) became available in the satellite era when both were repeatedly measured using altimetry, interferometry, and gravimetry (Bamber et al., 2018). This is a very short period to account for response time and to separate signals of climate change from impacts of climatic variability (Wouters et al., 2013). Modeling of SMB and glacial isostatic adjustment, analyses of ice cores and examination of geological evidence are used to put the recent changes in

perspective (Hanna et al., 2013). There have been more than 150 assessments of mass loss from the AIS and numerous assessments for the GrIS and inevitably, the estimates refer to different time periods, use different methods and are characterized by a large spread of values (Meredith et al., 2019). Numerous peripheral glaciers and ice caps surround both the AIS and the GrIS margins and changes in their mass balance can be considered together or separately from the ice sheets (see, e.g., Hock et al., 2019; Meredith et al., 2019). For Greenland, they account for a significant proportion of changes in ice mass (Bolch et al., 2013). Recently, independently derived estimates, based on the uniform assessment periods, were collated by the IMBIE project for the AIS (1992–2017) (The IMBIE Team, 2018) and the GrIS (1992–2018) (The IMBIE Team, 2020). These and other assessments are reviewed by Meredith et al. (2019).

4.1 Antarctic ice sheet

The AIS contains enough water to raise the global sea level by 58 m if it melts (The IMBIE Team, 2018). Assessments of changes in mass of the AIS focus on three distinctly different regions: the East Antarctic ice sheet (EAIS), which covers about 85% of the total AIS area, the West Antarctic ice sheet (WAIS), and the Antarctic Peninsula (AP). The EAIS mostly rests on landmass although there are marine sectors with limited unstable areas. Its central part, the East Antarctic Plateau has an average elevation of about 3000 m a.s.l. and is the coldest place of Earth where the absolute minimum temperature of −89°C was registered at the Vostok station. Rising air temperatures, therefore, do not have a direct effect on mass balance as they remain below freezing, but they lead to higher atmospheric moisture-holding capacity and precipitation. Due to the very low temperatures, precipitation is also extremely low over the Eastern Antarctic Plateau, which accounts for most of the EAIS, and its prevailing type is the so-called diamond dust which forms in the very cold atmosphere. Precipitation caused by weather systems is rare but an order of magnitude higher. Accumulation is very low, less than 50 mm a^{-1}, and exhibits strong interannual variability. An increase in precipitation and snow accumulation was observed since the beginning of the 20th century and attributed to the observed atmospheric warming, although a shorter-term negative trend observed since 1979 should be noted (Medley and Thomas, 2019). Longer precipitation and accumulation records, derived from ice cores, do not show spatially coherent trends over the EAIS (Thomas et al., 2017).

The WAIS is predominantly a marine ice sheet grounded below the sea level with the seabed deepening inland. Due to this configuration, the WAIS is considerably more unstable than the EAIS (Bamber et al., 2018). Similarly to the WAIS, the AP also has regions satisfying instability criteria (ibid.) but its geography and climatic conditions are distinctly different. Both the WAIS and particularly the AP are high-accumulation areas with annual precipitation around 500 mm a^{-1} in the AP. Snow accumulation has increased since the beginning of the 20th century, following an earlier decline over the AP (Goodwin et al., 2016; Thomas et al., 2017; Medley and Thomas, 2019). Here, variability in precipitation and accumulation is linked to variability in atmospheric circulation associated with the El Nino-Southern Oscillation (ENSO) and the Pacific Decadal Oscillation (PDO) (Goodwin et al., 2016). The reduction in the extent of sea ice in the Bellingshausen Sea, observed in the 20th century, also plays an important part in increasing the availability of surface-level moisture which leads to an increase in accumulation (Thomas et al., 2017). Over the WAIS, changes in snow accumulation were balanced between the eastern and western sectors (Medley and Thomas, 2019).

Complex systems of tributary glaciers and ice streams transport ice from the interior regions to the ocean (Rignot et al., 2011). Ice shelves buttress 90% of the AIS outflow (Meredith et al., 2019). The unstable configuration around the WAIS and the AP enables rapid grounding line retreat, acceleration of ice flow, and mass loss to the ocean (Bamber et al., 2009; Wouters et al., 2015). These processes accelerate when the buttressing effect of ice shelves is weakened by their thinning. Ice shelves are vulnerable to atmospheric warming at their surface and to changing ocean temperatures at their bases. Acceleration of ice shelf thinning has been observed around the WAIS and the AP since the mid-1990s and particularly after 2003 (Mouginot et al., 2014; Pritchard et al., 2012; Paolo et al., 2015). In the Amundsen and Bellingshausen regions, some ice shelves have lost up to 18% of their thickness in less than two decades. At the same time, the total volume of the EAIS ice shelves increased followed by a moderate loss after 2003 (Paolo et al., 2015).

Therefore, climatic warming may increase snowfall and accumulation, especially in the continental interiors, but enhance glacier discharge at the coast where rising air and ocean temperatures erode the buttressing ice shelves. Assessments agree that since 1992, the EAIS (whose area is larger by an order of magnitude than the WAIS) has been close to balance or slightly gaining mass because of increasing precipitation while the smaller WAIS and AP have been losing mass through an increase in ice flow (dynamic thinning) at a greater rate (Bamber et al., 2018; Meredith et al., 2019; The IMBIE Team, 2018). The EAIS mass balance was estimated as $5 \pm 46\,\mathrm{Gt\,a^{-1}}$ in the 1992–2017 period by The IMBIE Team (2018) (Table 1). Other studies agree that there was no clear trend in the EAIS mass balance over the period of satellite records, and stress interannual variability and very large uncertainties in measurements, which exceed the central estimate. The flow of glaciers, draining the EAIS, has remained largely constant (Gardner et al., 2018).

All assessments agree that ice loss from the AIS was dominated by acceleration and rapid dynamic thinning of the WAIS outlet glaciers driven by the melting of ice shelves and the loss of the buttressing effect (Mouginot et al., 2014; Meredith et al., 2019). The WAIS ice loss increased from 53 ± 29 to $159 \pm 26\,\mathrm{Gt\,a^{-1}}$ between the first and final 5 years of the 1992–2017 period with an average rate of $-94 \pm 27\,\mathrm{Gt\,a^{-1}}$ (The IMBIE Team, 2018) (Table 1). The strongest loss occurred in the Amundsen Sea sector where acceleration of glacier flow resulted in a 77% increase in ice discharge since the 1970s (Mouginot et al., 2014). In the AP, the average rate of

TABLE 1 Mass balance of the Antarctic ice sheets ($\mathrm{Gt\,a^{-1}}$).

Region	1992–1997	1997–2002	2002–2007	2007–2012	2012–2017	1992–2017
EAIS	11 ± 58	8 ± 56	12 ± 43	23 ± 38	-28 ± 30	5 ± 46
WAIS	-53 ± 29	-41 ± 28	-65 ± 27	-148 ± 27	-159 ± 26	-94 ± 27
AP	-7 ± 13	-6 ± 13	-20 ± 15	-35 ± 17	-33 ± 16	-20 ± 15
AIS	-49 ± 67	-38 ± 64	-73 ± 53	-160 ± 50	-219 ± 43	-109 ± 56

Data are from The IMBIE Team, 2018. Mass balance of the Antarctic ice sheet from 1992 to 2017. Nature 558, 219–222. https://doi.org/10.1038/s41586-018-0179-y. See Bamber, J.L., Westaway, R.M., Marzeion, B., Wouters, B., 2018. The land ice contribution to sea level during the satellite era. Environ. Res. Lett. 13, 063008. https://doi.org/10.1088/1748-9326/aac2f0 and Meredith, M., Sommerkorn, M., Cassotta, S., Derksen, C., Ekaykin, A., Hollowed, A., Kofinas, G., Mackintosh, A., Melbourne-Thomas, J., Muelbert, M.M.C., Ottersen, G., Pritchard, H., Schuur, E.A.G., 2019. Polar Regions. In: Pörtner, H.-O., Roberts, D.C., Masson-Delmotte, V., Zhai, P., Tignor, M., Poloczanska, E., Mintenbeck, K., Alegría, A., Nicolai, M., Okem, A., Petzold, J., Rama, B., Weyer, N.M. (Eds.), IPCC Special Report on the Ocean and Cryosphere in a Changing Climate. IPCC, Geneva for a wider range of assessments.

ice loss was $20 \pm 15\,\mathrm{Gt\,a^{-1}}$ with an increase of about $15\,\mathrm{Gt\,a^{-1}}$ since 2000. Of 860 marine-terminating glaciers located in the AP, 90% retreated from their 1940s positions (Cook et al., 2014) confirming that negative trend in mass balance extends beyond the satellite record. Dynamic thinning in the Amundsen Sea Embayment and the western AP accounted for 88% of the increase in the AIS mass loss from 2008 to 2015 (Gardner et al., 2018). These losses were partially offset by changes in precipitation and accumulation. However, mass loss from the AIS observed between 1992 and 2017, amounting to $2720 \pm 1390\,\mathrm{Gt}$ of ice (The IMBIE Team, 2018), accounted for 70% of the century-long snow accumulation gain of $3815 \pm 1105\,\mathrm{Gt}$ (Medley and Thomas, 2019).

4.2 Greenland ice sheet

The GrIS occupies about $1.71 \times 10^6\,\mathrm{km^2}$ and if its total volume of $2850 \times 10^3\,\mathrm{km^3}$ is to melt, the GMSL will rise by 7.4 m (The IMBIE Team, 2020). Here, changes in air temperature directly control melt (which extended to the summit in 2012), and, together with variability in snow accumulation, SMB. The relative contributions of SMB and D vary in time and spatially (Meredith et al., 2019; Mouginot et al., 2019; The IMBIE Team, 2020).

The observed air temperature increase in the Arctic and sub-Arctic regions, amplified by the reduced sea-ice coverage (the Arctic or Polar Amplification), is among the largest in the world (Serreze and Barry, 2011). Analysis of ice cores suggested that the 2000–10 decade was the warmest in about 2000 years (Vinther et al., 2009; Masson-Delmotte et al., 2012). However, quantifying its impacts on the evolution of the GrIS mass balance on a centennial time scale and longer remains challenging because of data availability and quality (Khan et al., 2015; van den Broeke et al., 2017). Our understanding of changes in the GrIS mass, elevation, and area (including peripheral glaciers) improved when spaceborne (Section 3.2) and airborne (Koenig et al., 2016; Lewis et al., 2017) data became available in the 1990s. Airborne surveys in particular helped to resolve large discrepancies in surface accumulation data. The availability of meteorological data used in modeling and mass balance reconstructions improved from the 1950s with emergence of the meteorological reanalysis data sets. Climatic and mass balance reconstructions for earlier years relied on data from coastal stations and ice cores used in combination with regional climate and mass balance models. Observational data were too sparse to capture spatial variability in temperature and especially in precipitation in high-accumulation areas leading to uncertainties which obscured climatic signals. Aerial photography and historical maps were used to reconstruct changes in glacier area and surface elevation. Kjeldsen et al. (2015) used aerial imagery from the 1980s to map moraines and reconstruct the maximum extent of the GrIS at the end of the 19th century and build its only historical DEM.

Studies of the 19th–early 20th century changes in the GrIS climate and mass balance agree on the direction of the general trend but discrepancies between absolute values and decadal anomalies are large before the 1950s. Thus Box (2013) estimated that summer temperature increased by 1.6°C over Greenland between 1840 and 2010. Temperature reconstruction by Hanna et al. (2011) for 1870–2010 suggested a smaller increase because in their record, temperatures prior to the 1940s were considerably higher. Both records were in agreement from the 1950s confirming that temperatures in the 1990–2000s were the highest over the GrIS since records began. Box (2013) suggested that accumulation increased over the GrIS from the

mid-20th century in comparison with the 1840–1940 period and reconstruction by Fettweis et al. (2017) for 1900–2015 agrees. Hanna et al. (2011) reported an opposite trend. Both, Hanna et al. (2011) and Box (2013) showed a negative anomaly in SMB in the 1960s attributing it to low accumulation. These and other studies agree that the GrIS gained mass in the 1970–80s and overall, the 1960–90s was a period of relative stability. van den Broeke et al. (2016, 2017) calculated SMB as $400 \pm 70\,\mathrm{Gt\,a^{-1}}$ in 1961–90 and the 1996 value of ice discharge as $410 \pm 20\,\mathrm{Gt\,a^{-1}}$ showing that ice flow adjusted to mass balance forcing and that the GrIS had near zero mass balance within the bounds of uncertainty.

In the early 2000s, the GrIS experienced a shift to negative annual and cumulative mass balance (Hanna et al., 2013; Khan et al., 2015; Box et al., 2018; Bamber et al., 2018; Mouginot et al., 2019). Kjeldsen et al. (2015) estimated mass loss from the GrIS as $75.1 \pm 29.4\,\mathrm{Gt\,a^{-1}}$ in the 1900–83 period, $73.8 \pm 40.5\,\mathrm{Gt\,a^{-1}}$ in the 1983–2003 period, and $186.4 \pm 18.9\,\mathrm{Gt\,a^{-1}}$ between 2003 and 2010.

Satellite and mass balance modeling data showed a strongly negative trend in SMB between 1992 and 2018 (Table 2), with a strong increase in melt and runoff (van den Broeke et al., 2016; Bamber et al., 2018; The IMBIE Team, 2020) in line with extensive surface warming (Hall et al., 2013; McGrath et al., 2013; Orsi et al., 2017), aided by an increasing fraction of liquid precipitation (Box et al., 2018). Box (2013) estimated that meltwater production increased by 59% between 1840 and 2010. In the 1994–2013 period, runoff from the GrIS occurred at a level unprecedented over at least 350 years, being 33% and 50% higher than the 20th century and the 18th century means, respectively (Trusel et al., 2018).

After 2002, mass balance became significantly more negative than in the previous years including both, SMB and dynamic discharge (Bamber et al., 2018; The IMBIE Team, 2020) (Table 2). The IMBIE Team (2020) estimated that SMB (and indirect firn processes) and dynamic discharge contributed to mass loss in approximately equal measures between 1992 and 2018 while in earlier periods, about 60% of the mass loss was through ice discharge and 40% was from surface ablation (van den Broeke et al., 2016; Bamber et al., 2018; Mouginot et al., 2019). Due to a very strong surface melt, observed in the first decade of the 21st century and peaking in 2012, the input of these processes in recent imbalance is the other way round: change in surface melt was mainly responsible for the observed imbalance (Bamber et al., 2018). Ice discharge also increased following the acceleration of large outlet glaciers in the

TABLE 2 Mass balance of the Greenland Ice Sheet ($\mathrm{Gt\,a^{-1}}$).

Component	1992–1997	1997–2002	2002–2007	2007–2012	2012–2017	1992–2018
SMB	26 ± 35	-15 ± 36	-78 ± 36	-193 ± 37	-139 ± 38	-76 ± 16
Dynamic	-52 ± 44	-29 ± 50	-96 ± 47	-82 ± 46	-105 ± 47	-75 ± 21
Total	-26 ± 27	-44 ± 35	-174 ± 30	-275 ± 28	-244 ± 28	-150 ± 13

Data are from The IMBIE Team, 2020. Mass balance of the Greenland ice sheet from 1992 to 2018. Nature 579, 233–239. https://doi.org/10.1038/s41586-019-1855-2. See Bamber, J.L., Westaway, R.M., Marzeion, B., Wouters, B., 2018. The land ice contribution to sea level during the satellite era. Environ. Res. Lett. 13, 063008. https://doi.org/10.1088/1748-9326/aac2f0 and Meredith, M., Sommerkorn, M., Cassotta, S., Derksen, C., Ekaykin, A., Hollowed, A., Kofinas, G., Mackintosh, A., Melbourne-Thomas, J., Muelbert, M.M.C., Ottersen, G., Pritchard, H., Schuur, E.A.G., 2019. Polar Regions. In: Poörtner, H.-O., Roberts, D.C., Masson-Delmotte, V., Zhai, P., Tignor, M., Poloczanska, E., Mintenbeck, K., Alegría, A., Nicolai, M., Okem, A., Petzold, J., Rama, B., Weyer, N.M. (Eds.), IPCC Special Report on the Ocean and Cryosphere in a Changing Climate. IPCC, Geneva for a wider range of assessments.

southeast and northwest and ubiquitous retreat of glacier calving fronts at an increasing rate (King et al., 2020). While only several large glaciers accounted for half of the dynamically driven ice loss from the GrIS in the 2000s, many more contribute now (Mouginot et al., 2019). Overall, between 1992 and 2018, the GrIS lost 1964 ± 565 and 1938 ± 541 Gt of ice because of meteorological processes and due to the dynamic imbalance of glaciers, respectively (The IMBIE Team, 2020). Both atmospheric and ocean forcing control dynamic mass loss from the GrIS, and the declining suppression effect of glacier calving by sea ice is important too (O'Leary and Christoffersen, 2013; Khan et al., 2015; Meredith et al., 2019).

While the observed increase in mass loss is attributed to rising temperatures, attribution of the observed atmospheric warming is less certain. Natural climatic variability plays an important part in controlling the GrIS mass balance. Thus, in the first decade of the 21st century, frequent occurrence of the negative phase of the North Atlantic Oscillation (NAO) led to enhanced advection of warm air masses, high pressure and increased insolation, and a reduction in solid precipitation over the GrIS in summer (Masson-Delmotte et al., 2012; Fettweis et al., 2013; Bevis et al., 2019). About 70% of the 1993–2012 summer warming is attributed to the NAO (Fettweis et al., 2013). These factors enhanced melt leading to more negative SMB particularly along the south-western margin of the GrIS which has greater area of lower-elevation ice surface per unit length, gentler slope, and where surface melting occurs much farther inland (Khan et al., 2015). Record melt was registered in 2012 when it extended to the summit of the GrIS. However, the negative trend in SMB slowed down between 2013 and 2018 in response to changing NAO phase which brought about lower summer temperatures and higher precipitation (Bevis et al., 2019).

Various positive feedbacks amplify melt at the GrIS. A very important feedback is linked to the darkening of the surface of the ice sheet. More intensive summer melt is further amplified by an increase in the spatial extent and duration of wet snow and areas of bare ice which have lower albedo (Box et al., 2018; Ryan et al., 2019). Algal growth and decay and, to a lesser extent, deposition of dust from the ice sheet periphery and black carbon, transported from industrial regions, on snow and ice reduce albedo, increasing melt further (van den Broeke et al., 2017). Only about a half of surface melt runs off the GrIS. A considerable portion is stored in snow and firn aquifers which spread to higher elevations as air temperature increases. The potential of these aquifers to buffer runoff is reduced by firn densification and formation of ice layers which prevent drainage and promote the formation of water ponds on the surface. This also reduces albedo enhancing melt further (Steger et al., 2017).

The GrIS appears to be significantly out of equilibrium (van den Broeke et al., 2016, 2017) and the observed increase in ice discharge alone is sufficient for transition to a new state of persistent negative mass balance (King et al., 2020). There is a considerable difference between a very long time of 4200 years, which would be required for the GrIS mass balance to adjust to a hypothetic increase in accumulation under the warmer climate, and mass loss through surface melt and calving, which occurs on the time scale of decades, significantly outpacing potential gains (van den Broeke et al., 2016). When the ice sheet has lost its contact with the ocean ($D = 0$) and SMB becomes persistently negative resulting in negative total mass balance, the GrIS has reached a "tipping point" beyond which it will not be able to recover. At the current rate of ice loss, the tipping point could be reached by the mid-21st century although in the absence of reliable long-term data uncertainty surrounding this scenario is high (van den Broeke et al., 2016).

4.3 Glaciers and ice caps

A period of glacier advance, which started with the onset of the LIA in the 15th century and peaked in the 17th century, ended at the turn of the 20th century (Solomina et al., 2016b). In the 20th century and particularly in its second half, and in the 21st century the overwhelming pattern of glacier behavior was that of loss of mass, retreat, and thinning in response to climatic warming. The combined glaciological and geodetic measurements showed that globally, glacier mass change amounted to -9625 ± 7975 Gt during the 1961–2016 period (Zemp et al., 2019). Increase in air temperature is primarily responsible for the observed glacier wastage (Hock et al., 2019). However, there were considerable spatial and temporal variations in the rates of glacier mass loss (and much more rarely, gain) (Winkler et al., 2010) resulting from multiple and often interdependent factors creating complex patterns of glacier response to climate change.

4.3.1 Factors affecting regional variability in glacier behavior and their response to climate change

The geography of glaciers is varied—from the poles to the tropics—and geographical location affects vulnerability of glaciers to climate change. Geographical location controls exposure to positive temperatures and solar radiation. Much of the Antarctic is not exposed to positive temperatures and ice loss is not directly affected by its increase. By contrast, glaciers in warmer regions are vulnerable to even a small temperature increase. Examples include the glaciers of southern Europe, for example, the Pyrenees where glaciers remain only on the highest peaks (González Trueba et al., 2008), tropical Andes (Vuille et al., 2008; Rabatel et al., 2013), and the Papua province of Indonesia where the last remaining glaciers in the West Pacific were melting rapidly since the 1960s in response to rising temperatures augmented by ENSO events (Permana et al., 2019). Geographical location controls amount and seasonality of precipitation. The former is higher in maritime regions where it can compensate for glacier melt. The latter predetermines whether glaciers are of winter or summer accumulation type. For example, glaciers in the European Alps, Scandinavia, and the Caucasus lose mass in summer and accumulate snow between September and May. On the glaciers of much of the Tien Shan, Pamir, and in the monsoonal regions of the Himalayas precipitation peaks in summer at the same time with melt (summer accumulation type). Fraction of liquid precipitation, which depends on temperature, and interruptions of melt by solid precipitation are important factors controlling mass balance of these glaciers. For these reasons, glaciers affected by monsoon may be more vulnerable to climatic warming than the winter-accumulation glaciers (Fujita, 2008). The Arctic glaciers are affected too because their ablation season is short and summer snowfalls can reduce melt very significantly.

Elevation controls temperature and precipitation regimes, and their relation to glacier area. Glaciers positioned at higher elevations have a larger AAR which sustains accumulation and transfer of ice downstream. Such glaciers are able to dynamically respond to climate change by retreating to higher elevations and, therefore, they are less vulnerable. By contrast, glaciers located at lower elevations have lost large parts of their accumulation area with ELA approaching the uppermost glacier elevation. Difference between values of cumulative mass balance of glaciers with higher and lower maximum elevations was clearly demonstrated by the region-wide mass balance assessment in the European Alps (Davaze et al., 2020).

For example, the Careser glacier in the Italian Alps (one of the WGMS reference glaciers) has lost its accumulation zone and is in the state of decay, which is intensified by decreasing surface albedo and increased input of heat from the exposed rocks (Carturan et al., 2013). The same is observed on many lower-elevation glaciers in other regions of the European Alps (Paul et al., 2007) and in the lower-elevation mountain ranges located in very different climates, for example, in the Kodar Mountains in north-eastern Siberia (Shahgedanova et al., 2011; Stokes et al., 2013).

Since size and hypsometry of glaciers (and, consequently, glacier type) control their response time and sensitivity to climatic perturbations, it is always important to take into account the predominant glacier parameters when comparing rates of glacier change in different regions. Due to higher sensitivity and shorter response time, small glaciers currently often account for larger proportions of regional area and mass loss. For example, in the Swiss and Lombardy Alps, in the last two decades of the 20th century glaciers with individual areas less than 1 km^2, accounting for only 15% and 30% of the glacierized area, contributed 40% and 58% of total area loss, respectively (Paul et al., 2004; Citterio et al., 2007). This is also why some smaller, steeper, fast-response glaciers in the Southern Alps of New Zealand, such as the Franz Josef glacier, advanced slightly at the beginning of the 21st century in response to decadal-scale climatic variability (Fig. 4) while large glaciers did not (Winkler et al., 2010; Chinn et al., 2005). This general pattern, however, can be disrupted by other factors. For example, due to local topography, small cirque glaciers had lower wastage rates than larger glaciers in the Polar Urals because they were shaded by cirque walls while larger valley glaciers were exposed to solar radiation (Shahgedanova et al., 2012).

Presence of debris cover on glacier surface affects melt rates. A very thin debris layer (up to about 2 cm) enhances glacier melt by reducing the albedo of the surface, however, thicker debris insulate glacier surface and reduce melt (Benn et al., 2012). A thick debris cover can alter the ablation gradient pushing higher melt rates from the well-insulated glacier tongues to the middle of the ablation zone (ibid.). About 7% of the total area of mountain glaciers is covered by debris. It is present on 44% of Earth's glaciers and prominent on 15% and, importantly, it is most abundant at lower elevations where melt rates are higher (Herreid and Pellicciotti, 2020). Fig. 6 shows an example of a debris-covered glacier. Over half of supra-glacial debris cover is concentrated in Alaska and in the Karakorum-Hindukush region. It is widespread in the Himalayas and in Central Asia. The presence of debris cover on the Himalayan glaciers contributes to their inhomogeneous response to climate change (Bolch et al., 2012). A comparison of retreat rates of the debris-free and debris-covered monsoon-influenced glaciers in the Himalayas showed that 65% of the former were retreating while the latter had stable fronts (Scherler et al., 2011). There are numerous studies showing lower retreat rates of the debris-covered glaciers in different parts of the world (e.g., Winkler et al., 2010; Chinn et al., 2005). However, it should be noted that downwasting rather than retreat may be a predominant way in which the debris-covered glaciers respond to climatic warming and this signal and a difference to the response of the debris-free glaciers are not always detected especially over short periods of time (Kääb et al., 2012). Another complicating factor is the formation of supra-glacial and moraine-dammed lakes on the debris-covered glaciers which, once formed, increase melt (Benn et al., 2012). At present, the mechanisms through which debris cover affects glacier melt are known but its contribution to glacier response is not quantified sufficiently well (Pellicciotti et al., 2015).

FIG. 6 The Shkhelda glacier in the northern Caucasus has extensive debris cover.

The LAI—black carbon (BC) and desert dust—enhance glacier melt. BC, a product of incomplete combustion in industrial processes, wildfires, and domestic biofuel use, is by far the most efficient type of aerosol absorbing solar radiation, changing albedo of glacier surface, and warming the atmosphere (Flanner et al., 2007; Bond et al., 2013; Khan et al., 2017). The Fifth IPCC report estimated the at-surface forcing of BC as +0.04 (0.02–0.09) $W\,m^{-2}$. BC can be transported over long distances and deposited as far as on the Antarctic glaciers, in the Arctic and Alaska, and was detected on the surface of glaciers and in ice cores in the Himalayas and Tibet, Andes, Rockies and European Alps. In the polar regions of the Northern Hemisphere, the highest concentrations are found in the Russian Arctic, particularly in its western sector where there are more settlements and large industrial facilities, and also in the Canadian Arctic and Alaska (Doherty et al., 2010; Dou and Xiao, 2016). Among the mountain regions, the Himalayas and Tibetan plateau stand out because of the widespread use of coal by power stations in India, China, and Iran and a widespread use of biofuel by households in India and Nepal (Menon et al., 2010). Deposition of BC on glaciers peaks in winter and spring. The latter is climatologically important because it can cause earlier onset and more intensive snow melt on glacier surface (Bond et al., 2013). Observations in the Khumbu Valley in Nepal showed that snow melt can start three weeks earlier if concentrations of BC on snow reach 300 ppb in comparison with clean snow (Jacobi et al., 2015). Moreover, the spring maximum in deposition of BC coincides with a peak in dust storms in the Middle East (Hennen et al., 2019) and Central Asia

(Nobakht et al., 2019) and deposition of desert dust on glaciers. Although the effect of dust on snow melt is substantially lower than that of BC, large dust storms events can generate strong radiative forcing and enhance melt (Painter et al., 2012; Gautam et al., 2013). In Fig. 1, mineral dust deposited on the Djankuat glacier can be recognized by its characteristic brownish color. Desert dust serves as a vector for transportation of various substances including BC. Therefore, a combined effect of BC and dust and their interactions with other impurities on glacier surface (cryoconite, algae), changes in snow grain size and, importantly, presence of debris cover (which can negate their impacts) should be considered. These processes are complex. As with debris cover, it is possible to quantify their effects on melt of a glacier but it is difficult to assess their contribution to glacier wastage overall. What is known is that deposition of BC and dust explains some of the variability in glacier change in the Arctic and in the Himalayas. It can be expected to increase if wildfires and dust storms become more frequent with climate change.

Whether glaciers terminate on land or in water affects their dynamics and rates of change. The formation of lakes at glacier tongues usually results in an acceleration of their retreat. For example, Yang et al. (2020) showed that in the Kenai Peninsula in Alaska, glaciers terminating in lakes lost about 30% more mass than glaciers terminating on land (and also nearly three times as much as tidewater glaciers) between 1986 and 2016. However, tidewater glaciers terminating in the ocean exhibit much more complex behavior which is not controlled by climate change alone. Tidewater glaciers go through a cycle whereby slow advance, which can continue for many centuries, is followed by stable position of glacier tongues and by rapid retreat which can occur within a century or less or even at surging speed (Cuffey and Paterson, 2010). The Columbia Glacier in south-eastern Alaska which flows from the elevation of 3050 m a.s.l. to the inlet leading to the Prince William Sound is an example. The glacier advanced between the 15th and 19th century but started retreating in the 1980s losing about 1 km of its length per year (Pfeffer, 2003). This does not imply that changes in the extent of tidewater glaciers are not controlled or triggered by changes in climate. Indeed, a consistent pattern of retreat of outlet glaciers was observed across the entire Atlantic sector of the Arctic from Greenland to Novaya Zemlya between 1992 and 2010 (Carr et al., 2017). However, tidewater glaciers respond to the climate-driven changes in ocean heat advection, sea ice conditions, atmospheric warming, and changes in precipitation in a complex way. Even within the same region they can be out of sync with land-terminating and other tidewater glaciers, and exhibit more varied responses than land-terminating glaciers. Carr et al. (2014) analyzed changes in the position of glacier tongues in the north of Novaya Zemlya between 1992 and 2010 and found that while 90% of all studied glaciers retreated, the observed changes could not be directly attributed to atmospheric warming; correlations with sea ice conditions and SST were significant but not strong; and fjord geometry (a nonclimatic factor) was the most important control over variability between retreat rates of individual glaciers. These conclusions were re-iterated in a wider study of the Atlantic Arctic (Carr et al., 2017). McNabb and Hock (2014) examined changes in the positions of 50 tidewater glacier termini between 1948 and 2012 in Alaska and found that while 60% of the glaciers retreated overall, there was no coherent pattern of their retreats and advances and it was not clear whether retreats were triggered by increasing SST. Cook et al. (2019) investigated changes in more than 300 marine-terminating glaciers between 1958 and 2015 in the Canadian Arctic Archipelago, reporting gradual retreat before 2000 and a fivefold increase in retreat rates up to 2015. The latter was attributed to atmospheric warming driving retreat in the same way as that of land-terminating glaciers, in

contrast to other regions where the delivery of ocean heat was a stronger control over the retreat of marine-terminating glaciers.

Last but not least, interannual variability in atmospheric circulation is an important control over short-term glacier fluctuations which can enhance or temporarily obscure the long-term change. Decadal variability in mass balance of glaciers in the Andes, particularly in Bolivia, Ecuador, Columbia and to a lesser extent in Peru, is governed by SST variability in the Pacific. Here glaciers respond strongly to the ENSO cycle with El Niño years featuring a strongly negative mass balance and La Niña events producing a nearly balanced or even slightly positive mass balance (Vuille et al., 2008; Rabatel et al., 2013). The NAO controls variability in glacier mass balance in western Scandinavia. Rapid glacier advances during the positive NAO phases, which result in abundant winter precipitation in this region, were recorded throughout the LIA (Nesje and Dahl, 2003) and in the 20th century, especially in the 1990s when maritime glaciers in Norway experienced a mass gain and advanced (Nesje et al., 2000; Chinn et al., 2005; Paul and Andreassen, 2009). In the Southern Alps of New Zealand, glaciers with short response time advanced between the 1980s and 2000 (Fig. 4) in response to change in the Interdecadal Pacific Oscillation which occurred in 1976/77 and continued until 1998 (Chinn et al., 2005).

4.3.2 Changes in mass and extent of glaciers

Despite regional variations and exceptions, there is a coherent global pattern of glacier retreat. Glacier length records from all continents and almost all latitudes show that glaciers receded worldwide since the start of the 20th century (Leclercq et al., 2014) (Fig. 4). Numerous regional analyses of glacier area change and their compilations show glacier shrinkage especially since the second half of the 20th century (Pfeffer et al., 2014; Kargel et al., 2014). Glacier mass change reconstructions for the 20th century also agree on glacier mass loss rates (Leclercq et al., 2011; Marzeion et al., 2015). Zemp et al. (2019) estimated an increase in mean global glacier mass loss by approximately 30% between 1986 and 2005 and 2006 and 2015.

The best data are available for 2006–15 and Table 3 summarizes glacier mass balance of mountain and polar glaciers for this common assessment period (Hock et al., 2019; Meredith et al., 2019). Due to the large ice extent, the highest glacier mass loss occurred in Alaska, the Greenland periphery and the Canadian Arctic and in the mountain regions, in the Southern Andes (including the Patagonian ice fields) and the HMA. A comparison of the specific mass balance (loss per unit area) shows that they were comparable in the Arctic and in the mountains in 2006–15 at $-500 \pm 70\,\mathrm{kg\,m^{-2}\,a^{-1}}$ and $-490 \pm 100\,\mathrm{kg\,m^{-2}\,a^{-1}}$, respectively (Hock et al., 2019). In the Arctic, glaciers of the southern sector of the Canadian Arctic had the most negative specific mass balance at $-800 \pm 220\,\mathrm{kg\,m^{-2}\,a^{-1}}$ followed by Alaska, while in Svalbard it was $-270 \pm 170\,\mathrm{kg\,m^{-2}\,a^{-1}}$ (Hock et al., 2019). Among the mountain regions, the most negative averages (less than $-850\,\mathrm{kg\,m^{-2}\,a^{-1}}$) were observed in the Southern Andes, Caucasus, European Alps, and Pyrenees. The European Alps were losing mass at a rate of $-910 \pm 70\,\mathrm{kg\,m^{-2}\,a^{-1}}$ in 2006–15 (Table 3) and this trend is a part of longer, widespread glacier wastage across the entire European Alps (Sommer et al., 2020) (Fig. 4). The least negative mass budget characterized the High Mountain Asia where it averaged $-140 \pm 110\,\mathrm{kg\,m^{-2}\,a^{-1}}$.

On a multidecadal time scale, the largest cumulative mass loss was observed from Alaska accounting for about a third of the total change of $-8305 \pm 5115\,\mathrm{Gt}$ from all glaciers, excluding the peripheries of Antractica and Greenland between 1961 and 2016 (Zemp et al., 2019). All other assessments agree that Alaska is a hotspot of glacier change (Jacob et al., 2012;

TABLE 3 Regional estimates of glacier mass budget in the common assessment period of 2006–15 by the IPCC Special Report on Ocean and Cryosphere in a Changing Climate (SROCC) (Hock et al., 2019). Regional glacier areas and volumes are from RGI Consortium (2017) and Farinotti et al. (2019). Regions of assessment are as in RGI Consortium (2017). "Arctic Total" values include Alaska, Iceland, and Scandinavia which are also included in "Mountains Total".

Mass budget	Area	Volume	Mass budget		
Region	km^2	mm SLE	$Gt\,a^{-1}$	$kg\,m^{-2}\,a^{-1}$	mm SLE a^{-1}
Antarctic periphery	132,867	69.4 ± 18	−11 ± 108	−90 ± 860	0.03 ± 0.3
Greenland periphery	89,717	33.6 ± 8.7	−47 ± 16	−570 ± 200	0.13 ± 0.04
Arctic Canada North	105,111	64.8 ± 16.8	−39 ± 8	−380 ± 80	0.11 ± 0.02
Arctic Canada South	40,888	20.5 ± 5.3	−33 ± 9	−800 ± 220	0.09 ± 0.03
Western Canada and USA	14,524	2. 6 ± 0.7	−8 ± 13	−500 ± 910	0.02 ± 0.04
Alaska	86,725	43.3 ± 11.2	−60 ± 16	−700 ± 180	0.17 ± 0.04
Iceland	11,060	9.1 ± 2.4	−7 ± 3	−690 ± 260	0.02 ± 0.01
Svalbard	33,959	17.3 ± 4.5	−9 ± 5	−270 ± 170	0.02 ± 0.01
Russian Arctic	51,592	32.0 ± 8.3	−15 ± 12	−300 ± 270	0.04 ± 0.03
High Mountain Asia	97,605	16.9 ± 2.7	−14 ± 11	−150 ± 110	0.04 ± 0.03
Southern Andes	29,429	12.8 ± 3.3	−25 ± 4	−860 ± 170	0.07 ± 0.01
Central Europe	2092	0.3 ± 0.1	−2 ± 0	−910 ± 70	0.01 ± 0.00
Scandinavia	2949	0.7 ± 0.2	−2 ± 1	−660 ± 270	0.01 ± 0.00
Caucasus and Middle East	1307	0.2 ± 0.0	−1 ± 1	−880 ± 570	0.00 ± 0.00
Northern Asia	2410	0.3 ± 0.1	−1 ± 1	−400 ± 310	0.00 ± 0.00
New Zealand	1162	0.2 ± 0.0	−1 ± 1	−590 ± 1140	0.00 ± 0.00
Low latitudes	23,41	0.2 ± 0.1	−1 ± 1	−590 ± 580	0.00 ± 0.00
Arctic total	422,000	221 ± 25	−213 ± 29	−500 ± 70	0.59 ± 0.08
Mountains total	251,604	87 ± 15	−123 ± 24	−490 ± 100	0.34 ± 0.07
Global total	705,739	324 ± 84	−278 ± 113	−390 ± 160	0.77 ± 0.31

Data are from Hock, R., Rasul, G., Adler, C., Cáceres, B., Gruber, S., Hirabayashi, Y., Jackson, M., Kääb, A., Kang, S., Kutuzov, S., Milner, A., Molau, U., Morin, S., Orlove, B., Steltzer, H., 2019. High Mountain Areas. In: Poörtner, H.-O., Roberts, D.C., Masson-Delmotte, V., Zhai, P., Tignor, M., Poloczanska, E., Mintenbeck, K., Alegría, A.,Nicolai, M., Okem, A., Petzold, J., Rama, B., Weyer, N.M. (Eds.), IPCC Special Report on the Ocean and Cryosphere in a Changing Climate. IPCC, Geneva. Also see the reference for other assessments.

Gardner et al., 2013; Box et al., 2018). Most of the ice loss occurred in the southern coastal part of the region and surface melt strongly dominated over tidewater glacier retreat (Larsen et al., 2015). The largest reduction in specific cumulative mass balance was observed in the Southern Andes resulting in total mass loss of 1200 Gt, which is less than in Alaska where the total glacierized area is three times higher (Table 3). Other assessments of glacier change in the Southern Andes show that the loss of glacier area has continued since the LIA with the Northern and Southern Patagonian Icefields losing over 100 km^2 and 500 km^2 of

glacierized area since their maximum extent in 1870 and 1650, respectively (Glasser et al., 2011). The centennial rates of mass loss were an order of magnitude lower than in the second half of the 20th century.

In the HMA, very strong spatial variations in the response of glaciers to climate change were observed (Azam et al., 2018). Brun et al. (2017) reported contrasting regional trends in 2000–16 varying from the strongly negative mass balance in Nyainqentanglha, Tibet ($-620 \pm 230\,\mathrm{kg\,m^{-2}\,a^{-1}}$) through moderately negative in the Himalayas (ranging from $-420 \pm 200\,\mathrm{kg\,m^{-2}\,a^{-1}}$ in Bhutan to $-330 \pm 200\,\mathrm{kg\,m^{-2}\,a^{-1}}$ in eastern Nepal) to slightly positive in the Kunlun Mountains ($+140 \pm 80\,\mathrm{kg\,m^{-2}\,a^{-1}}$). Glaciers in the western and central Pamir exhibited low mass losses and in the eastern Pamir they had balanced budgets (Brun et al., 2017; Bolch et al., 2019). Detected originally in the Karakoram, where regional mass budgets were nearly balanced since the 1970s (Azam et al., 2018), this unusual pattern was termed the Karakoram Anomaly although at present the highest increases in ice mass are registered over the eastern part of the Karakoram and the western Kunlun. Various explanations were suggested ranging from the widespread occurrence of surging glaciers and extensive debris cover to climatic controls and even anthropogenic influence (Azam et al., 2018; Farinotti et al., 2020). Archer and Fowler (2004) identified negative trends in summer and annual temperatures, and an increase in summer, winter and annual precipitation over the Karakoram in 1961–2000 while Treydte et al. (2006) showed that the 20th century was the wettest in the last millennium. These changes are consistent with increase in mass balance. Attributions of the observed trends in precipitation include the impact of the NAO, the strengthening of the westerly jet stream, the main mechanism of moisture delivery (Archer and Caldeira, 2008; Cannon et al., 2014; Norris et al., 2019), and interactions with the Karakoram/West Tibet Vortex (Forsythe et al., 2017; Li et al., 2018) while regional cooling in the 1960–80 period appears to be influenced by the weakening monsoon (ibid.). Another suggested explanation is a dramatic expansion of irrigation in China (Cook et al., 2015) which caused an increase in evaporation and cloud cover and, consequently, decrease in solar radiation and more frequent summer snowfalls over the western Kunlun and Pamir (Bashir et al., 2017; Norris et al., 2019). This hypothesis is plausible but requires further investigation. Sakai and Fujita (2017) argued that not only climatic trends but also the higher mass balance sensitivity of regional glaciers to climatic forcing is behind the observed mass gain. Given the importance of the state of regional glaciers to water supply and glacier-related hazards, it is important to understand the mechanisms creating the Karakoram-Kunlun-Pamir anomaly.

5 Contribution to global mean sea level change

Perhaps the main impact of the observed glacier melt and projected future glacier change is their contribution to GMSL rise. It is estimated that up to 187 million people could be displaced by a GMSL rise of 1 m and the aggressive climate change scenarios in the future (Nicholls et al., 2011) but costs to coastal population, infrastructure, agricultural land and ecosystems can be immense even under more restrained scenarios (Oppenheimer et al., 2019). Observed changes in sea level are derived from a global network of tide gauges (with some records starting as early as the 1700s) and, at present, from satellite altimetry (Church et al., 2011). Contributions from different sources are calculated. Under the warming climate,

GMSL rise is caused by the expanding volume of the ocean due to lower density of warmer water (thermal expansion), increase in the mass of the ocean caused by the loss of land ice, and net changes in other terrestrial water reservoirs, for example, ground water depletion (Church et al., 2011; Oppenheimer et al., 2019).

There are several assessments of glacier melt contribution to GMSL rise. Cogley (2009) and Zemp et al. (2019) used glaciological and geodetic records of mass balance to calculate its input for 2000–05 and 1961–2016, respectively. Oerlemans et al. (2007) and Leclercq et al. (2011) used data on glacier front variations as proxies for volume change to reconstruct input of glaciers to GMSL rise in 1850–2000 and 1800–2005, respectively. Marzeion et al. (2012) reconstructed glacier input to GMSL rise for 1900–2005 from meteorological records calibrated with mass balance data and this work was extended by Marzeion et al. (2015). Gardner et al. (2013) used ICESat altimetry to assess input of glaciers to GMSL rise in 2003–09. There were substantial variations between the earlier assessments because of uncertainties associated with upscaling of mass balance records, which are not uniformly distributed throughout the world, and modeling (e.g., important processes such as calving were not explicitly included). Uncertainties in assessments based on glacier length resulted from the fact that change in glacier length is a function of length itself and that glaciers can lose mass through thinning while their tongues remain nearly stagnant. Rapid extension of geodetic mass balance assessments from spaceborne data alleviated many of these problems (Zemp et al., 2019).

Reliable assessments of contributions of ice sheets to GMSL rise became available with frequent satellite observations in the 1990s with further improvements in data quality in the 2000s, when GRACE data became available. Multimethod assessments were produced by Gardner et al. (2013), Bamber et al. (2018), Wouters et al. (2019), and IMBIE (The IMBIE Team, 2018, 2020). Estimations of ice sheet contribution to GMSL in the 20th century were attempted based on the combined use of modeling and tide gauge records (Hay et al., 2015) and geodetic reconstruction of the GrIS since 1900 by Kjeldsen et al. (2015).

TABLE 4 Global mean sea level budget derived from observations ($mm\,a^{-1}$). Numbers in parentheses are uncertainties ranging from 5% to 95%.

Source	1901–1990	1970–2015	1993–2015	2006–2015
Thermal expansion		0.89 (0.84–0.94)	1.36 (0.96–1.76)	1.40 (1.08–1.72)
Glaciers	0.49 (0.34–0.64)	0.46 (0.21–0.72)	0.56 (0.34–0.78)	0.61 (0.53–0.69)
GrIS and peripheral glaciers	0.40 (0.23–0.57)		0.46 (0.21–0.71)	0.77 (0.72–0.82)
AIS and peripheral glaciers			0.29 (0.11–0.47)	0.43 (0.34–0.52)
Land water storage	−0.12	−0.07	0.09	−0.21 (−0.36–0.06)
Total			2.76 (2.21–3.31)	3.00 (2.62–3.38)
Tide gauge and altimetry records	1.38 (0.81–1.95)	2.06 (1.77–2.34)	3.16 (2.79–3.53)	3.58 (3.10–4.06)

Data are from Oppenheimer, M., Glavovic, B.C., Hinkel, J., van de Wal, R., Magnan, A.K., Abd-Elgawad, A., Cai, R., CifuentesJara, M., DeConto, R.M., Ghosh, T., Hay, J., Isla, F., Marzeion, B., Meyssignac, B., Sebesvari, Z., 2019. Sea level rise and implications for low-lying islands, coasts and communities. In: Poörtner, H.-O., Roberts, D.C., Masson-Delmotte, V., Zhai, P., Tignor, M., Poloczanska, E., Mintenbeck, K., Alegría, A., Nicolai, M., Okem, A., Petzold, J., Rama, B., Weyer , N.M. (Eds.), IPCC Special Report on the Ocean and Cryosphere in a Changing Climate. IPCC, Geneva. See their Table 4.1 and accompanying text for a detailed explanation of how different components of GMSL were obtained.

Observed changes in and contribution to GMSL change were summarized by Oppenheimer et al. (2019) for four time periods according to data availability (Table 4). The 1993–2015 and 2006–15 periods are short and might be affected by climatic variability. The 2006–15 assessments are based on improved data coverage and methods.

In 1993–2015, thermal expansion and contribution from glaciers were the largest contributors to the observed GMSL rise, accounting for 43% and 20%, respectively, while Greenland and Antarctica contributed 15% and 9%. In 2006–15, the observed sea level rise accelerated and the combined input of land ice became the main contributor over thermal expansion with glaciers, Greenland and Antarctica contributing 20%, 21%, and 12%, respectively. Although Antarctica contains eight times more ice above flotation than Greenland, the latter currently provides the largest input in GMSL rise. Glacier melt in the Canadian Arctic, Alaska, and the Southern Andes were the largest contributors among the Arctic and mountain glaciers (Table 3). Box et al. (2018) estimated that over a longer time period of 1971–2013, Alaska's contribution to GMSL rise was 1.8 times higher than that of the Canadian Arctic because of the earlier onset of continuing ice loss. Overall, the Arctic is a very significant contributor to GMSL rise.

6 Synthesis and outlook

Assessments of climate and glacier change agree that accelerated wastage of glaciers was observed in the 20th century and increasing loss of ice mass occurred from the GrIS, the AP, and the WAIS in the last few decades. The observed loss of ice can be confidently attributed to the continuing climatic warming. Due to the observed imbalance between the current glacier mass and climate, a large loss of glacier area and mass are expected in the mountain and polar regions in the future (Hock et al., 2019). Future changes in the extent of glaciers and ice sheets and their contributions to GMSL change depend on which representative concentration pathway (RCP) or emission scenario is followed. However, sea level rise is expected to be faster at the end of the 21st century under all scenarios including those compatible with achieving the long-term temperature goal set out in the Paris Agreement.

Global glacier mass loss between 2015 and 2100 is expected to reach 18% (with a range of 11%–25%) for the least aggressive RCP2.6 scenario and 36% (26%–47%) for the most aggressive RCP8.5 scenario. This corresponds to 94 (69–119) mm and 200 (156–240) mm of sea level rise, respectively. Mountain ranges, dominated by small glaciers, such as the European Alps, Pyrenees, Caucasus, North Asia and tropical regions, may lose more than 80% of their ice cover, however, the Arctic region and Antarctic periphery are expected to be the main contributors to GMSL rise (Hock et al., 2019). While the direction of the global trend is clear, the magnitude and timing of ice loss are subject to large uncertainties. These originate from the uncertainty in climate scenarios but also from many unknowns in glaciological models, such as the omission of mass loss by iceberg calving, subaqueous melt processes and instability mechanisms, from most global studies.

A likely range of the GrIS contribution to GMSL rise by the end of the 21st century is 4–10 cm under RCP2.6 and 7–21 cm under RCP8.5 (Oppenheimer et al., 2019). Surface melt and runoff are expected to dominate over ice discharge. Greenland's bedrock topography, whereby there is limited contact between thick ice and the ocean, is expected to limit the potential pace of GMSL rise from GrIS (ibid.). Evolution of the AIS is characterized by deep

uncertainties. At the upper end of RCP8.5, Antarctica can contribute up to 28 cm of sea level rise by the end of the 21st century and the instability of the WAIS and its peripheral marine-terminating glaciers is expected to make the most significant impact. Potential loss of ice from the EAIS could make a major contribution to sea level in the future because of its vast extent (Oppenheimer et al., 2019).

Glacier wastage can affect regional water availability especially in the arid regions where glaciers are important sources of water, such as Central Asia and the Andes (Huss and Hock, 2018). Streamflow in glacier-fed rivers shows distinct seasonality with a pronounced maximum in the melt season which can coincide either with the wet season (e.g., monsoon-dominated regions where changes in glacier runoff make less impact on water availability) or with the dry season (e.g., Hindukush, Karakoram, Central Asia where impacts can be significant). At present, runoff is increasing in many glacierized catchments because water is released from long-term storage (glacier ice) until maximum or so-called peak water is reached. Afterwards, runoff will decline because the diminished glacier area will not be able to support high flow rates. Knowledge about the timing of peak water as well as reliable estimations of future changes in runoff are important for the development of adaptation strategies. Many regional assessments exist, for example, Juen et al. (2007) for the Cordillera Blanca, Farinotti et al. (2012) for the Swiss Alps, Immerzeel et al. (2012) for the Nepalese Himalayas, Lutz et al. (2014) for the HMA, Ragettli et al. (2016) for the Himalayas and the Andes, Duethmann et al. (2015, 2016), and Shahgedanova et al. (2018, 2020) for the Tien Shan, and many others. These studies and a global assessment by Huss and Hock (2018) showed that peak water is expected in the middle of the 21st century in the HMA (with an earlier peak in the outer ranges of the Tien Shan and later in the Indus headwaters) but in the Alps and the Andes, it has passed or is expected in the next decade. Changes in glacier runoff can have many consequences beyond water availability, for example, too much water can lead to the formation of glacier lakes and GLOF, too little to deterioration of water quality. Many of these impacts are reviwed by Huss et al. (2017) and Hock et al. (2019).

The global cryosphere is declining and this trend is expected to continue. The global community of scientists is working on assessments of the past, and prediction of the future, changes and their impacts, but a different intiative is under way. The Ice Memory Project under the auspices of UNESCO is building the first world archive of hundreds of ice cores in the ice cave at the Antarctica's Concordia research station, where mean annual temperature is about −54 °C, to preserve ice for generations of future researchers.

References

Archer, C.L., Caldeira, K., 2008. Historical trends in the jet streams. Geophys. Res. Lett. 35, L08803. https://doi.org/10.1029/2008GL033614.

Archer, D.R., Fowler, H.J., 2004. Spatial and temporal variations in precipitation in the Upper Indus Basin, global teleconnections and hydrological implications. Hydrol. Earth Syst. Sci. 8, 47–61. https://doi.org/10.5194/hess-8-47-2004.

Azam, M.F., Wagnon, P., Berthier, E., Vincent, C., Fujita, K., Kargel, J.S., 2018. Review of the status and mass changes of Himalayan-Karakoram glaciers. J. Glaciol. 64 (243), 61–74. https://doi.org/10.1017/jog.2017.86.

Bamber, J.L., Riva, R.E.M., Vermeersen, B.L.A., LeBrocq, A.M., 2009. Reassessment of the potential sea-level rise from a collapse of the West Antarctic ice sheet. Science 324, 901–903. https://doi.org/10.1126/science.1169335.

Bamber, J.L., Westaway, R.M., Marzeion, B., Wouters, B., 2018. The land ice contribution to sea level during the satellite era. Environ. Res. Lett. 13, 063008. https://doi.org/10.1088/1748-9326/aac2f0.

Barandun, M., Huss, M., Usubaliev, R., Azisov, E., Berthier, E., Kääb, A., Bolch, T., Hoelzle, M., 2018. Multi-decadal mass balance series of three Kyrgyz glaciers inferred from modelling constrained with repeated snow line observations. Cryosphere 12, 1899–1919. https://doi.org/10.5194/tc-12-1899-2018.

Bashir, F., Zeng, X., Gupta, H., Hazenberg, P., 2017. A Hydrometeorological perspective on the Karakoram anomaly using unique valley-based synoptic weather observations. Geophys. Res. Lett. 44, 10,470–10,478. https://doi.org/10.1002/2017GL075284.

Benn, D.I., Bolch, T., Hands, K., Gulley, J., Luckman, A., Nicholson, L.I., Quincey, D., Thompson, S., Toumi, R., Wiseman, S., 2012. Response of debris-covered glaciers in the Mount Everest region to recent warming, and implications for outburst flood hazards. Earth Sci. Rev. 114, 156–174. https://doi.org/10.1016/j.earscirev.2012.03.008.

Berthier, E., Vincent, C., Magnússon, E., Gunnlaugsson, P., Pitte, P., Le Meur, E., Masiokas, M., Ruiz, L., Pálsson, F., Belart, J.M.C., Wagnon, P., 2014. Glacier topography and elevation changes derived from Pléiades sub-meter stereo images. Cryosphere 8, 2275–2291. https://doi.org/10.5194/tc-8-2275-2014.

Bevis, M., Harig, C., Khan, S.A., Brown, A., Simons, F.J., Willis, M., Fettweis, X., Van Den Broeke, M.R., Madsen, F.B., Kendrick, E., Caccamise, D.J., Van Dam, T., Knudsen, P., Nylen, T., 2019. Accelerating changes in ice mass within Greenland, and the ice sheet's sensitivity to atmospheric forcing. Proc. Natl. Acad. Sci. U. S. A. 116, 1934–1939. https://doi.org/10.1073/pnas.1806562116.

Bhambri, R., Bolch, T., 2009. Glacier mapping: a review with special reference to the Indian Himalayas. Prog. Phys. Geogr. 33, 672–704. https://doi.org/10.1177/0309133309348112.

Bolch, T., Kulkarni, A., Kääb, A., Huggel, C., Paul, F., Cogley, J.G., Frey, H., Kargel, J.S., Fujita, K., Scheel, M., Bajracharya, S., Stoffel, M., 2012. The state and fate of Himalayan glaciers. Science 336, 310–314. https://doi.org/10.1126/science.1215828.

Bolch, T., Sandberg Sørensen, L., Simonsen, S.B., Mölg, N., Machguth, H., Rastner, P., Paul, F., 2013. Mass loss of Greenland's glaciers and ice caps 2003-2008 revealed from ICESat laser altimetry data. Geophys. Res. Lett. 40, 875–881. https://doi.org/10.1002/grl.50270.

Bolch, T., Shea, J.M., Liu, S., Azam, F.M., Gao, Y., Gruber, S., Immerzeel, W.W., Kulkarni, A., Li, H., Tahir, A.A., Zhang, G., Zhang, Y., 2019. Status and change of the cryosphere in the extended Hindu Kush Himalaya region. In: The Hindu Kush Himalaya Assessment. Springer International Publishing, Cham, pp. 209–255. https://doi.org/10.1007/978-3-319-92288-1_7.

Bond, T.C., Doherty, S.J., Fahey, D.W., Forster, P.M., Berntsen, T., DeAngelo, B.J., Flanner, M.G., Ghan, S., Kärcher, B., Koch, D., Kinne, S., Kondo, Y., Quinn, P.K., Sarofim, M.C., Schultz, M.G., Schulz, M., Venkataraman, C., Zhang, H., Zhang, S., Bellouin, N., Guttikunda, S.K., Hopke, P.K., Jacobson, M.Z., Kaiser, J.W., Klimont, Z., Lohmann, U., Schwarz, J.P., Shindell, D., Storelvmo, T., Warren, S.G., Zender, C.S., 2013. Bounding the role of black carbon in the climate system: a scientific assessment. J. Geophys. Res. Atmos. 118, 5380–5552. https://doi.org/10.1002/jgrd.50171.

Box, J.E., 2013. Greenland ice sheet mass balance reconstruction. Part II. Surface mass balance (1840–2010). J. Clim. 26, 6974–6989. https://doi.org/10.1175/JCLI-D-12-00518.1.

Box, J.E., Colgan, W.T., Wouters, B., Burgess, D.O., O'Neel, S., Thomson, L.I., Mernild, S.H., 2018. Global Sea-level contribution from Arctic land ice: 1971–2017. Environ. Res. Lett. 13, 125012. https://doi.org/10.1088/1748-9326/aaf2ed.

Brun, F., Berthier, E., Wagnon, P., Kääb, A., Treichler, D., 2017. A spatially resolved estimate of High Mountain Asia glacier mass balances, 2000–2016. Nat. Geosci. 10, 668–673. https://doi.org/10.1038/NGEO2999.A.

Cannon, F., Carvalho, L.M.V., Jones, C., Bookhagen, B., 2014. Multi-annual variations in winter westerly disturbance activity affecting the Himalaya. Clim. Dyn. 44, 441–455. https://doi.org/10.1007/s00382-014-2248-8.

Carr, J.R., Stokes, C., Vieli, A., 2014. Recent retreat of major outlet glaciers on Novaya Zemlya, Russian Arctic, influenced by fjord geometry and sea-ice conditions. J. Glaciol. 60, 155–170. https://doi.org/10.3189/2014JoG13J122.

Carr, J.R., Stokes, C.R., Vieli, A., 2017. Threefold increase in marine-terminating outlet glacier retreat rates across the Atlantic Arctic: 1992–2010. Ann. Glaciol. 58, 72–91. https://doi.org/10.1017/aog.2017.3.

Carturan, L., Baroni, C., Becker, M., Bellin, A., Cainelli, O., Carton, A., Casarotto, C., Dalla Fontana, G., Godio, A., Martinelli, T., Salvatore, M.C., Seppi, R., 2013. Decay of a long-term monitored glacier: Careser glacier (Ortles-Cevedale, European Alps). Cryosphere 7, 1819–1838. https://doi.org/10.5194/tc-7-1819-2013.

Chinn, T., Winkler, S., Salinger, M.J., Haakensen, N., 2005. Recent glacier advances in Norway and New Zealand: a comparison of their glaciological and meteorological causes. Geogr. Ann. Ser. A Phys. Geogr. 87, 141–157. https://doi.org/10.1111/j.0435-3676.2005.00249.x.

Church, J.A., White, N.J., Konikow, L.F., Domingues, C.M., Cogley, J.G., Rignot, E., Gregory, J.M., van den Broeke, M.R., Monaghan, A.J., Velicogna, I., 2011. Revisiting the Earth's sea-level and energy budgets from 1961 to 2008. Geophys. Res. Lett. 38. https://doi.org/10.1029/2011GL048794.

Citterio, M., Diolaiuti, G., Smiraglia, C., D'agata, C., Carnielli, T., Stella, G., Siletto, G.B., 2007. The fluctuations of italian glaciers during the last century: a contribution to knowledge about alpine glacier changes. Geogr. Ann. Ser. A Phys. Geogr. 89, 167–184. https://doi.org/10.1111/j.1468-0459.2007.00316.x.

Cogley, J.G., 2009. Geodetic and direct mass-balance measurements: comparison and joint analysis. Ann. Glaciol. 50, 96–100. https://doi.org/10.3189/172756409787769744.

Cook, A.J., Copland, L., Noël, B.P.Y., Stokes, C.R., Bentley, M.J., Sharp, M.J., Bingham, R.G., van den Broeke, M.R., 2019. Atmospheric forcing of rapid marine-terminating glacier retreat in the Canadian Arctic archipelago. Sci. Adv. 5, eaau8507. https://doi.org/10.1126/sciadv.aau8507.

Cook, A.J., Vaughan, D.G., Luckman, A.J., Murray, T., 2014. A new Antarctic peninsula glacier basin inventory and observed area changes since the 1940s. Antarct. Sci. 26, 614–624. https://doi.org/10.1017/S0954102014000200.

Cook, B.I., Shukla, S.P., Puma, M.J., Nazarenko, L.S., 2015. Irrigation as an historical climate forcing. Clim. Dyn. 44, 1715–1730. https://doi.org/10.1007/s00382-014-2204-7.

Cuffey, K.M., Paterson, W.S.B., 2010. The Physics of Glaciers. Elsevier, Oxford.

Davaze, L., Rabatel, A., Dufour, A., Hugonnet, R., Arnaud, Y., 2020. Region-wide annual glacier surface mass balance for the European Alps from 2000 to 2016. Front. Earth Sci. 8, 1–14. https://doi.org/10.3389/feart.2020.00149.

Doherty, S.J., Warren, S.G., Grenfell, T.C., Clarke, A.D., Brandt, R.E., 2010. Light-absorbing impurities in Arctic snow. Atmos. Chem. Phys. 10, 11647–11680. https://doi.org/10.5194/acp-10-11647-2010.

Dou, T.-F., Xiao, C.-D., 2016. An overview of black carbon deposition and its radiative forcing over the Arctic. Adv. Clim. Chang. Res. 7, 115–122. https://doi.org/10.1016/j.accre.2016.10.003.

Duethmann, D., Bolch, T., Farinotti, D., Kriegel, D., Vorogushyn, S., Merz, B., Pieczonka, T., Jiang, T., Su, B., Güntner, A., 2015. Attribution of streamflow trends in snow and glacier melt-dominated catchments of the Tarim River, Central Asia. Water Resour. Res. 51, 4727–4750. https://doi.org/10.1002/2014WR016716.

Duethmann, D., Menz, C., Jiang, T., Vorogushyn, S., 2016. Projections for headwater catchments of the Tarim River reveal glacier retreat and decreasing surface water availability but uncertainties are large. Environ. Res. Lett. 11, 1–13. https://doi.org/10.1088/1748-9326/11/5/054024.

Farinotti, D., Huss, M., Fürst, J.J., Landmann, J., Machguth, H., Maussion, F., Pandit, A., 2019. A consensus estimate for the ice thickness distribution of all glaciers on Earth. Nat. Geosci. 12. https://doi.org/10.1038/s41561-019-0300-3.

Farinotti, D., Immerzeel, W.W., de Kok, R.J., Quincey, D.J., Dehecq, A., 2020. Manifestations and mechanisms of the Karakoram glacier anomaly. Nat. Geosci. 13, 8–16. https://doi.org/10.1038/s41561-019-0513-5.

Farinotti, D., Usselmann, S., Huss, M., Bauder, A., Funk, M., 2012. Runoff evolution in the Swiss Alps: projections for selected high-alpine catchments based on ENSEMBLES scenarios. Hydrol. Process. 26, 1909–1924. https://doi.org/10.1002/hyp.8276.

Fettweis, X., Box, J.E., Agosta, C., Amory, C., Kittel, C., Lang, C., Van As, D., Machguth, H., Gallée, H., 2017. Reconstructions of the 1900-2015 Greenland ice sheet surface mass balance using the regional climate MAR model. Cryosphere 11, 1015–1033. https://doi.org/10.5194/tc-11-1015-2017.

Fettweis, X., Hanna, E., Lang, C., Belleflamme, A., Erpicum, M., Gallée, H., 2013. Brief communication important role of the mid-tropospheric atmospheric circulation in the recent surface melt increase over the Greenland ice sheet. Cryosphere 7, 241–248. https://doi.org/10.5194/tc-7-241-2013.

Flanner, M.G., Zender, C.S., Randerson, J.T., Rasch, P.J., 2007. Present-day climate forcing and response from black carbon in snow. J. Geophys. Res. 112, 1–17. https://doi.org/10.1029/2006JD008003.

Forsythe, N., Fowler, H.J., Li, X.-F., Blenkinsop, S., Pritchard, D., 2017. Karakoram temperature and glacial melt driven by regional atmospheric circulation variability. Nat. Clim. Chang. 7, 664–670. https://doi.org/10.1038/nclimate3361.

Fujita, K., 2008. Effect of precipitation seasonality on climatic sensitivity of glacier mass balance. Earth Planet. Sci. Lett. 276, 14–19. https://doi.org/10.1016/j.epsl.2008.08.028.

Gardner, A.S., Moholdt, G., Cogley, J.G., Wouters, B., Arendt, A.A., Wahr, J., Berthier, E., Hock, R., Pfeffer, W.T., Kaser, G., Ligtenberg, S.R.M., Bolch, T., Sharp, M.J., Hagen, J.O., van den Broeke, M.R., Paul, F., 2013.

A reconciled estimate of glacier contributions to sea level rise: 2003 to 2009. Science 340, 852–857. https://doi.org/10.1126/science.1234532.
Gardner, A.S., Moholdt, G., Scambos, T., Fahnstock, M., Ligtenberg, S., van den Broeke, M., Nilsson, J., 2018. Increased West Antarctic and unchanged East Antarctic ice discharge over the last 7 years. Cryosphere 12, 521–547. https://doi.org/10.5194/tc-12-521-2018.
Gautam, R., Hsu, N.C., Lau, W.K., Yasunari, T.J., 2013. Satellite observations of desert dust-induced Himalayan snow darkening. Geophys. Res. Lett. 40, 988–993. https://doi.org/10.1002/GRL.50226.
Glasser, N.F., Harrison, S., Jansson, K.N., Anderson, K., Cowley, A., 2011. Global sea-level contribution from the Patagonian icefields since the little ice age maximum. Nat. Geosci. 4, 303–307. https://doi.org/10.1038/ngeo1122.
González Trueba, J.J., Moreno, R.M., Martínez de Pisón, E., Serrano, E., 2008. 'Little Ice Age' glaciation and current glaciers in the Iberian Peninsula. The Holocene 18, 551–568. https://doi.org/10.1177/0959683608089209.
Goodwin, B.P., Mosley-Thompson, E., Wilson, A.B., Porter, S.E., Roxana Sierra-Hernandez, M., 2016. Accumulation variability in the Antarctic peninsula: the role of large-scale atmospheric oscillations and their interactions. J. Clim. 29, 2579–2596. https://doi.org/10.1175/JCLI-D-15-0354.1.
Haeberli, W., 1995. Glacier fluctuations and climate change detection. Geogr. Fis. Din. Quat. 191–199.
Haeberli, W., Linsbauer, A., 2013. Global glacier volumes and sea level—small but systematic effects of ice below the surface of the ocean and of new local lakes on land. Cryosphere 7, 817–821. https://doi.org/10.5194/tc-7-817-2013.
Haeberli, W., Whiteman, C. (Eds.), 2015. Snow and Ice-Related Hazards, Risks, and Disasters. Elsevier, Oxford.
Hall, D.K., Comiso, J.C., DiGirolamo, N.E., Shuman, C.A., Box, J.E., Koenig, L.S., 2013. Variability in the surface temperature and melt extent of the Greenland ice sheet from MODIS. Geophys. Res. Lett. 40, 2114–2120. https://doi.org/10.1002/grl.50240.
Hanna, E., Huybrechts, P., Cappelen, J., Steffen, K., Bales, R.C., Burgess, E., McConnell, J.R., Peder Steffensen, J., Van den Broeke, M., Wake, L., Bigg, G., Griffiths, M., Savas, D., 2011. Greenland ice sheet surface mass balance 1870 to 2010 based on twentieth century reanalysis, and links with global climate forcing. J. Geophys. Res. Atmos. 116. https://doi.org/10.1029/2011JD016387.
Hanna, E., Navarro, F.J., Pattyn, F., Domingues, C.M., Fettweis, X., Ivins, E.R., Nicholls, R.J., Ritz, C., Smith, B., Tulaczyk, S., Whitehouse, P.L., Zwally, H.J., 2013. Ice-sheet mass balance and climate change. Nature 498, 51–59. https://doi.org/10.1038/nature12238.
Hay, C.C., Morrow, E., Kopp, R.E., Mitrovica, J.X., 2015. Probabilistic reanalysis of twentieth-century sea-level rise. Nature 517, 481–484. https://doi.org/10.1038/nature14093.
Hennen, M., White, K., Shahgedanova, M., 2019. An assessment of SEVIRI imagery at various temporal resolutions and the effect on accurate dust emission mapping. Remote Sens. 11. https://doi.org/10.3390/rs11080965.
Herreid, S., Pellicciotti, F., 2020. The state of rock debris covering Earth's glaciers. Nat. Geosci. 13. https://doi.org/10.1038/s41561-020-0615-0.
Hock, R., Rasul, G., Adler, C., Cáceres, B., Gruber, S., Hirabayashi, Y., Jackson, M., Kääb, A., Kang, S., Kutuzov, S., Milner, A., Molau, U., Morin, S., Orlove, B., Steltzer, H., 2019. High Mountain Areas. In: Poörtner, H.-O., Roberts, D.C., Masson-Delmotte, V., Zhai, P., Tignor, M., Poloczanska, E., Mintenbeck, K., Alegría, A., Nicolai, M., Okem, A., Petzold, J., Rama, B., Weyer, N.M. (Eds.), IPCC Special Report on the Ocean and Cryosphere in a Changing Climate. IPCC, Geneva.
Huss, M., 2013. Density assumptions for converting geodetic glacier volume change to mass change. Cryosphere 7, 877–887. https://doi.org/10.5194/tc-7-877-2013.
Huss, M., Bookhagen, B., Huggel, C., Jacobsen, D., Bradley, R.S., Clague, J.J., Vuille, M., Buytaert, W., Cayan, D.R., Greenwood, G., Mark, B.G., Milner, A.M., Weingartner, R., Winder, M., 2017. Toward mountains without permanent snow and ice. Earth's Future 5, 418–435. https://doi.org/10.1002/eft2.207.
Huss, M., Hock, R., 2018. Global-scale hydrological response to future glacier mass loss. Nat. Clim. Chang. 8, 135–140. https://doi.org/10.1038/s41558-017-0049-x.
Immerzeel, W.W., van Beek, L.P.H., Konz, M., Shrestha, A.B., Bierkens, M.F.P., 2012. Hydrological response to climate change in a glacierized catchment in the Himalayas. Clim. Chang. 110, 721–736. https://doi.org/10.1007/s10584-011-0143-4.
IPCC, 2019. IPCC Special Report on the Ocean and Cryosphere in a Changing Climate. IPCC, Geneva.
Jacob, T., Wahr, J., Pfeffer, W.T., Swenson, S., 2012. Recent contributions of glaciers and ice caps to sea level rise. Nature 482, 514–518. https://doi.org/10.1038/nature10847.

Jacobi, H.-W., Lim, S., Ménégoz, M., Ginot, P., Laj, P., Bonasoni, P., Stocchi, P., Marinoni, A., Arnaud, Y., 2015. Black carbon in snow in the upper Himalayan Khumbu Valley, Nepal: observations and modeling of the impact on snow albedo, melting, and radiative forcing. Cryosphere 9, 1685–1699. https://doi.org/10.5194/tc-9-1685-2015.

Juen, I., Kaser, G., Georges, C., 2007. Modelling observed and future runoff from a glacierized tropical catchment (Cordillera Blanca, Perú). Glob. Planet. Chang. 59, 37–48. https://doi.org/10.1016/j.gloplacha.2006.11.038.

Kääb, A., Berthier, E., Nuth, C., Gardelle, J., Arnaud, Y., 2012. Contrasting patterns of early twenty-first-century glacier mass change in the Himalayas. Nature 488, 495–498. https://doi.org/10.1038/nature11324.

Kapitsa, V., Shahgedanova, M., MacHguth, H., Severskiy, I., Medeu, A., 2017. Assessment of evolution and risks of glacier lake outbursts in the Djungarskiy Alatau, Central Asia, using Landsat imagery and glacier bed topography modelling. Nat. Hazards Earth Syst. Sci. 17. https://doi.org/10.5194/nhess-17-1837-2017.

Kapitsa, V., Shahgedanova, M., Severskiy, I., Kasatkin, N., White, K., Usmanova, Z., 2020. Assessment of changes in mass balance of the Tuyuksu Group of Glaciers, northern Tien Shan, between 1958 and 2016 using ground-based observations and Pléiades satellite imagery. Front. Earth Sci. 8. https://doi.org/10.3389/feart.2020.00259.

Kargel, J.S., Leonard, G.J., Bishop, M.P., Kaab, A., Raup, B., 2014. Global Land Ice Measurements From Space. Springer-Praxis.

Kaser, G., Großhauser, M., Marzeion, B., Barry, R.G., 2010. Contribution potential of glaciers to water availability in different climate regimes. Proc. Natl. Acad. Sci. U. S. A. 107, 21300–21305. https://doi.org/10.1073/pnas.

Kaser, G., Hardy, D.R., Mölg, T., Bradley, R.S., Hyera, T.M., 2004. Modern glacier retreat on Kilimanjaro as evidence of climate change: observations and facts. Int. J. Climatol. 24, 329–339. https://doi.org/10.1002/joc.1008.

Khan, A.L., Wagner, S., Jaffe, R., Xian, P., Williams, M., Armstrong, R., McKnight, D., 2017. Dissolved black carbon in the global cryosphere: concentrations and chemical signatures. Geophys. Res. Lett. 44, 6226–6234. https://doi.org/10.1002/2017GL073485.

Khan, S.A., Aschwanden, A., Bjørk, A.A., Wahr, J., Kjeldsen, K.K., Kjær, K.H., 2015. Greenland ice sheet mass balance: a review. Rep. Prog. Phys. 78, 046801. https://doi.org/10.1088/0034-4885/78/4/046801.

King, M.D., Howat, I.M., Candela, S.G., Noh, M.J., Jeong, S., Noël, B.P.Y., van den Broeke, M.R., Wouters, B., Negrete, A., 2020. Dynamic ice loss from the Greenland ice sheet driven by sustained glacier retreat. Commun. Earth Environ. 1, 1. https://doi.org/10.1038/s43247-020-0001-2.

Kjeldsen, K.K., Korsgaard, N.J., Bjørk, A.A., Khan, S.A., Box, J.E., Funder, S., Larsen, N.K., Bamber, J.L., Colgan, W., van den Broeke, M., Siggaard-Andersen, M.-L., Nuth, C., Schomacker, A., Andresen, C.S., Willerslev, E., Kjær, K.H., 2015. Spatial and temporal distribution of mass loss from the Greenland ice sheet since AD 1900. Nature 528, 396–400. https://doi.org/10.1038/nature16183.

Koenig, L.S., Ivanoff, A., Alexander, P.M., MacGregor, J.A., Fettweis, X., Panzer, B., Paden, J.D., Forster, R.R., Das, I., McConnell, J.R., Tedesco, M., Leuschen, C., Gogineni, P., 2016. Annual Greenland accumulation rates (2009–2012) from airborne snow radar. Cryosphere 10, 1739–1752. https://doi.org/10.5194/tc-10-1739-2016.

Kutuzov, S., Lavrentiev, I., Smirnov, A., Nosenko, G., 2019. Volume changes of Elbrus glaciers from 1997 to 2017. Front. Earth Sci. 7, 153. https://doi.org/10.3389/feart.2019.00153.

Kutuzov, S., Shahgedanova, M., 2009. Glacier retreat and climatic variability in the eastern Terskey-Alatoo, inner Tien Shan between the middle of the 19th century and beginning of the 21st century. Glob. Planet. Chang. 69. https://doi.org/10.1016/j.gloplacha.2009.07.001.

Larsen, C.F., Burgess, E., Arendt, A.A., O'Neel, S., Johnson, A.J., Kienholz, C., 2015. Surface melt dominates Alaska glacier mass balance. Geophys. Res. Lett. 42, 5902–5908. https://doi.org/10.1002/2015GL064349.

Leclercq, P.W., Oerlemans, J., Basagic, H.J., Bushueva, I., Cook, A.J., Le Bris, R., 2014. A data set of worldwide glacier length fluctuations. Cryosphere 8, 659–672. https://doi.org/10.5194/tc-8-659-2014.

Leclercq, P.W., Oerlemans, J., Cogley, J.G., 2011. Estimating the glacier contribution to sea-level rise for the period 1800–2005. Surv. Geophys. 32, 519–535. https://doi.org/10.1007/s10712-011-9121-7.

Lewis, G., Osterberg, E., Hawley, R., Whitmore, B., Marshall, H.P., Box, J., 2017. Regional Greenland accumulation variability from operation IceBridge airborne accumulation radar. Cryosphere 11, 773–788. https://doi.org/10.5194/tc-11-773-2017.

Li, X.F., Fowler, H.J., Forsythe, N., Blenkinsop, S., Pritchard, D., 2018. The Karakoram/Western Tibetan vortex: seasonal and year-to-year variability. Clim. Dyn. 51, 3883–3906. https://doi.org/10.1007/s00382-018-4118-2.

Loriaux, T., Casassa, G., 2013. Evolution of glacial lakes from the northern Patagonia icefield and terrestrial water storage in a sea-level rise context. Glob. Planet. Chang. 102, 33–40. https://doi.org/10.1016/j.gloplacha.2012.12.012.

Lutz, A.F., Immerzeel, W.W., Shrestha, A.B., Bierkens, M.F.P., 2014. Consistent increase in high Asia's runoff due to increasing glacier melt and precipitation. Nat. Clim. Chang. 4. https://doi.org/10.1038/NCLIMATE2237.

Marzeion, B., Champollion, N., Haeberli, W., Langley, K., Leclercq, P., Paul, F., 2017. Observation-based estimates of global glacier mass change and its contribution to sea-level change. Surv. Geophys. 38, 105–130. https://doi.org/10.1007/s10712-016-9394-y.

Marzeion, B., Jarosch, A.H., Hofer, M., 2012. Past and future sea-level change from the surface mass balance of glaciers. Cryosphere 6, 1295–1322. https://doi.org/10.5194/tc-6-1295-2012.

Marzeion, B., Leclercq, P.W., Cogley, J.G., Jarosch, A.H., 2015. Brief communication: global reconstructions of glacier mass change during the 20th century are consistent. Cryosphere 9, 2399–2404. https://doi.org/10.5194/tc-9-2399-2015.

Masson-Delmotte, V., Swingedouw, D., Landais, A., Seidenkrantz, M.-S., Gauthier, E., Bichet, V., Massa, C., Perren, B., Jomelli, V., Adalgeirsdottir, G., Hesselbjerg Christensen, J., Arneborg, J., Bhatt, U., Walker, D.A., Elberling, B., Gillet-Chaulet, F., Ritz, C., Gallée, H., van den Broeke, M., Fettweis, X., de Vernal, A., Vinther, B., 2012. Greenland climate change: from the past to the future. Wiley Interdiscip. Rev. Clim. Chang. 3, 427–449. https://doi.org/10.1002/wcc.186.

McGrath, D., Colgan, W., Bayou, N., Muto, A., Steffen, K., 2013. Recent warming at summit, Greenland: global context and implications. Geophys. Res. Lett. 40, 2091–2096. https://doi.org/10.1002/grl.50456.

McNabb, R.W., Hock, R., 2014. Alaska tidewater glacier terminus positions, 1948–2012. J. Geophys. Res. Earth Surf. 119, 153–167. https://doi.org/10.1002/2013JF002915.

Medley, B., Thomas, E.R., 2019. Increased snowfall over the Antarctic ice sheet mitigated twentieth-century sea-level rise. Nat. Clim. Chang. 9, 34–39. https://doi.org/10.1038/s41558-018-0356-x.

Menon, S., Koch, D., Beig, G., Sahu, S., Fasullo, J., Orlikowski, D., 2010. Black carbon aerosols and the third polar ice cap. Atmos. Chem. Phys. 10, 4559–4571. https://doi.org/10.5194/acp-10-4559-2010.

Meredith, M., Sommerkorn, M., Cassotta, S., Derksen, C., Ekaykin, A., Hollowed, A., Kofinas, G., Mackintosh, A., Melbourne-Thomas, J., Muelbert, M.M.C., Ottersen, G., Pritchard, H., Schuur, E.A.G., 2019. Polar Regions. In: -Poörtner, H.-O., Roberts, D.C., Masson-Delmotte, V., Zhai, P., Tignor, M., Poloczanska, E., Mintenbeck, K., Alegría, A., Nicolai, M., Okem, A., Petzold, J., Rama, B., Weyer, N.M. (Eds.), IPCC Special Report on the Ocean and Cryosphere in a Changing Climate. IPCC, Geneva.

Mölg, T., Cullen, N.J., Hardy, D.R., Kaser, G., Klok, L., 2008. Mass balance of a slope glacier on Kilimanjaro and its sensitivity to climate. Int. J. Climatol. 28, 881–892. https://doi.org/10.1002/joc.1589.

Mouginot, J., Rignot, E., Bjørk, A.A., van den Broeke, M., Millan, R., Morlighem, M., Noël, B., Scheuchl, B., Wood, M., 2019. Forty-six years of Greenland ice sheet mass balance from 1972 to 2018. Proc. Natl. Acad. Sci. 116, 9239–9244. https://doi.org/10.1073/pnas.1904242116.

Mouginot, J., Rignot, E., Scheuchl, B., 2014. Sustained increase in ice discharge from the Amundsen sea embayment, West Antarctica, from 1973 to 2013. Geophys. Res. Lett. 41, 1576–1584. https://doi.org/10.1002/2013GL059069.

Nesje, A., Dahl, S.O., 2003. The 'Little Ice Age'—only temperature? The Holocene 13, 139–145. https://doi.org/10.1191/0959683603hl603fa.

Nesje, A., Lie, O., Dahl, S.O., 2000. Is the North Atlantic oscillation reflected in Scandinavian glacier mass balance records? J. Quat. Sci. 15, 587–601. https://doi.org/10.1002/1099-1417(200009)15:6<587::AID-JQS533>3.0.CO;2-2.

Nicholls, R.J., Marinova, N., Lowe, J.A., Brown, S., Vellinga, P., de Gusmão, D., Hinkel, J., Tol, R.S.J., 2011. Sea-level rise and its possible impacts given a 'beyond 4°C world' in the twenty-first century. Philos. Trans. R. Soc. A Math. Phys. Eng. Sci. 369, 161–181. https://doi.org/10.1098/rsta.2010.0291.

Nobakht, M., Shahgedanova, M., White, K., 2019. New inventory of dust sources in Central Asia derived from the daily MODIS imagery. E3S Web Conf. 99, 01001. https://doi.org/10.1051/e3sconf/20199901001.

Norris, J., Carvalho, L.M.V., Jones, C., Cannon, F., 2019. Deciphering the contrasting climatic trends between the central Himalaya and Karakoram with 36 years of WRF simulations. Clim. Dyn. 52, 159–180. https://doi.org/10.1007/s00382-018-4133-3.

O'Leary, M., Christoffersen, P., 2013. Calving on tidewater glaciers amplified by submarine frontal melting. Cryosphere 7, 119–128. https://doi.org/10.5194/tc-7-119-2013.

Oerlemans, J., 2010. Extracting a climate signal from 169 glacier records. Science 308 (5722), 675–677. https://doi.org/10.1126/science.1107046.

Oerlemans, J., Dyurgerov, M., van de Wal, R.S.W., 2007. Reconstructing the glacier contribution to sea-level rise back to 1850. Cryosphere 1, 59–65. https://doi.org/10.5194/tc-1-59-2007.

Oppenheimer, M., Glavovic, B.C., Hinkel, J., van de Wal, R., Magnan, A.K., Abd-Elgawad, A., Cai, R., CifuentesJara, M., DeConto, R.M., Ghosh, T., Hay, J., Isla, F., Marzeion, B., Meyssignac, B., Sebesvari, Z., 2019. Sea level rise and implications for low-lying islands, coasts and communities. In: Poörtner, H.-O., Roberts, D.C., Masson-Delmotte, V., Zhai, P., Tignor, M., Poloczanska, E., Mintenbeck, K., Alegría, A.,

Nicolai, M., Okem, A., Petzold, J., Rama, B., Weyer, N.M. (Eds.), IPCC Special Report on the Ocean and Cryosphere in a Changing Climate. IPCC, Geneva.
Orsi, A.J., Kawamura, K., Masson-Delmotte, V., Fettweis, X., Box, J.E., Dahl-Jensen, D., Clow, G.D., Landais, A., Severinghaus, J.P., 2017. The recent warming trend in North Greenland. Geophys. Res. Lett. 44, 6235–6243. https://doi.org/10.1002/2016GL072212.
Painter, T.H., Bryant, A.C., Skiles, S.M., 2012. Radiative forcing by light absorbing impurities in snow from MODIS surface reflectance data. Geophys. Res. Lett. 39. https://doi.org/10.1029/2012GL052457.
Paolo, F.S., Fricker, H.A., Padman, L., 2015. Volume loss from Antarctic ice shelves is accelerating. Science 348, 327–331. https://doi.org/10.1126/science.aaa0940.
Paul, F., Andreassen, L.M., 2009. A new glacier inventory for the Svartisen region, Norway, from Landsat ETM + data: challenges and change assessment. J. Glaciol. 55, 607–618.
Paul, F., Kääb, A., Haeberli, W., 2007. Recent glacier changes in the Alps observed by satellite: consequences for future monitoring strategies. Glob. Planet. Chang. 56, 111–122. https://doi.org/10.1016/j.gloplacha.2006.07.007.
Paul, F., Kääb, A., Maisch, M., Kellenberger, T., Haeberli, W., 2004. Rapid disintegration of alpine glaciers observed with satellite data. Geophys. Res. Lett. 31. https://doi.org/10.1029/2004GL020816.
Pellicciotti, F., Stephan, C., Miles, E., Herreid, S., Immerzeel, W.W., Bolch, T., 2015. Mass-balance changes of the debris-covered glaciers in the Langtang Himal, Nepal, from 1974 to 1999. J. Glaciol. 61, 373–386. https://doi.org/10.3189/2015JoG13J237.
Pepin, N., Bradley, R.S., Diaz, H.F., Baraer, M., Caceres, E.B., Forsythe, N., Fowler, H., Greenwood, G., Hashmi, M.Z., Liu, X.D., Miller, J.R., Ning, L., Ohmura, A., Palazzi, E., Rangwala, I., Schöner, W., Severskiy, I., Shahgedanova, M., Wang, M.B., Williamson, S.N., Yang, D.Q., 2015. Elevation-dependent warming in mountain regions of the world. Nat. Clim. Chang. 5, 424–430. https://doi.org/10.1038/nclimate2563.
Permana, D.S., Thompson, L.G., Mosley-Thompson, E., Davis, M.E., Lin, P.-N., Nicolas, J.P., Bolzan, J.F., Bird, B.W., Mikhalenko, V.N., Gabrielli, P., Zagorodnov, V., Mountain, K.R., Schotterer, U., Hanggoro, W., Habibie, M.N., Kaize, Y., Gunawan, D., Setyadi, G., Susanto, R.D., Fernández, A., Mark, B.G., 2019. Disappearance of the last tropical glaciers in the Western Pacific warm Pool (Papua, Indonesia) appears imminent. Proc. Natl. Acad. Sci. 116, 26382–26388. https://doi.org/10.1073/pnas.1822037116.
Pfeffer, W.T., 2003. Tidewater glaciers move at their own pace. Nature 426, 602. https://doi.org/10.1038/426602a.
Pfeffer, W.T., Arendt, A.A., Bliss, A., Bolch, T., Cogley, J.G., Gardner, A.S., Hagen, J.-O., Hock, R., Kaser, G., Kienholz, C., Miles, E.S., Moholdt, G., Mölg, N., Paul, F., Radić, V., Rastner, P., Raup, B.H., Rich, J., Sharp, M.J., 2014. The Randolph glacier inventory: a globally complete inventory of glaciers. J. Glaciol. 60, 537–552. https://doi.org/10.3189/2014JoG13J176.
Pieczonka, T., Bolch, T., 2015. Region-wide glacier mass budgets and area changes for the central Tien Shan between ~1975 and 1999 using hexagon KH-9 imagery. Glob. Planet. Chang. 128, 1–13. https://doi.org/10.1016/j.gloplacha.2014.11.014.
Pritchard, H.D., Ligtenberg, S.R.M., Fricker, H.A., Vaughan, D.G., Van Den Broeke, M.R., Padman, L., 2012. Antarctic ice-sheet loss driven by basal melting of ice shelves. Nature 484, 502–505. https://doi.org/10.1038/nature10968.
Rabatel, A., Francou, B., Soruco, A., Gomez, J., Cáceres, B., Ceballos, J.L., Basantes, R., Vuille, M., Sicart, J.-E., Huggel, C., Scheel, M., Lejeune, Y., Arnaud, Y., Collet, M., Condom, T., Consoli, G., Favier, V., Jomelli, V., Galarraga, R., Ginot, P., Maisincho, L., Mendoza, J., Ménégoz, M., Ramirez, E., Ribstein, P., Suarez, W., Villacis, M., Wagnon, P., 2013. Current state of glaciers in the tropical Andes: a multi-century perspective on glacier evolution and climate change. Cryosphere 7, 81–102. https://doi.org/10.5194/tc-7-81-2013.
Radić, V., Hock, R., 2010. Regional and global volumes of glaciers derived from statistical upscaling of glacier inventory data. J. Geophys. Res. 115, F01010. https://doi.org/10.1029/2009JF001373.
Ragettli, S., Immerzeel, W.W., Pellicciotti, F., 2016. Contrasting climate change impact on river flows from high-altitude catchments in the Himalayan and Andes Mountains. Proc. Natl. Acad. Sci. U. S. A. 113, 9222–9227. https://doi.org/10.1073/pnas.1606526113.
Raup, B., Ka, A., Kargel, J.S., Bishop, M.P., Hamilton, G., Lee, E., Paul, F., Rau, F., Soltesz, D., Jodha, S., Khalsa, S., Beedle, M., Helm, C., 2007. Remote sensing and GIS technology in the Global Land Ice Measurements from Space (GLIMS) Project. Comput. Geosci. 33, 104–125. https://doi.org/10.1016/j.cageo.2006.05.015.
RGI Consortium, 2017. Randolph Glacier Inventory—A Dataset of Global Glacier Outlines: Version 6.0R: Technical Report. Global Land Ice Measurements from Space, Colorado, USAhttps://doi.org/10.7265/N5-RGI-60.
Rignot, E., 1996. Tidal motion, ice velocity and melt rate of Petermann Gletscher, Greenland, measured from radar interferometry. J. Glaciol. 42, 476–485. https://doi.org/10.1017/S0022143000003464.

Rignot, E., Mouginot, J., Scheuchl, B., 2011. Ice flow of the Antarctic ice sheet. Science 333, 1427–1430. https://doi.org/10.1126/science.1208336.

Ryan, J.C., Smith, L.C., van As, D., Cooley, S.W., Cooper, M.G., Pitcher, L.H., Hubbard, A., 2019. Greenland ice sheet surface melt amplified by snowline migration and bare ice exposure. Sci. Adv. 5, eaav3738. https://doi.org/10.1126/sciadv.aav3738.

Sakai, A., Fujita, K., 2017. Contrasting glacier responses to recent climate change in high-mountain Asia. Sci. Rep. 7, 1–8. https://doi.org/10.1038/s41598-017-14256-5.

Scherler, D., Bookhagen, B., Strecker, M.R., 2011. Spatially variable response of Himalayan glaciers to climate change affected by debris cover. Nat. Geosci. 4, 156–159. https://doi.org/10.1038/ngeo1068.

Serreze, M.C., Barry, R.G., 2011. Processes and impacts of Arctic amplification: a research synthesis. Glob. Planet. Chang. 77, 85–96. https://doi.org/10.1016/j.gloplacha.2011.03.004.

Shahgedanova, M., Afzal, M., Hagg, W., Kapitsa, V., Kasatkin, N., Mayr, E., Rybak, O., Saidaliyeva, Z., Severskiy, I., Usmanova, Z., Wade, A., Yaitskaya, N., Zhumabayev, D., 2020. Emptying water towers? Impacts of future climate and glacier change on river discharge in the northern Tien Shan, Central Asia. Water 12 (3), 627. https://doi.org/10.3390/w12030627.

Shahgedanova, M., Afzal, M., Severskiy, I., Usmanova, Z., Saidaliyeva, Z., Kapitsa, V., Kasatkin, N., Dolgikh, S., 2018. Changes in the mountain river discharge in the northern Tien Shan since the mid-20th century: results from the analysis of a homogeneous daily streamflow data set from seven catchments. J. Hydrol. 564, 1133–1152. https://doi.org/10.1016/j.jhydrol.2018.08.001.

Shahgedanova, M., Nosenko, G., Bushueva, I., Ivanov, M., 2012. Changes in area and geodetic mass balance of small glaciers, polar Urals, Russia, 1950–2008. J. Glaciol. 58, 953–964. https://doi.org/10.3189/2012JoG11J233.

Shahgedanova, M., Popovnin, V., Aleynikov, A., Stokes, C.R., 2011. Geodetic mass balance of Azarova glacier, Kodar mountains, eastern siberia, and its links to observed and projected climatic change. Ann. Glaciol. 52 (58), 129–137. https://doi.org/10.3189/172756411797252275.

Solomina, O., Bushueva, I., Dolgova, E., Jomelli, V., Alexandrin, M., Mikhalenko, V., Matskovsky, V., 2016a. Glacier variations in the northern Caucasus compared to climatic reconstructions over the past millennium. Glob. Planet. Chang. 140, 28–58. https://doi.org/10.1016/j.gloplacha.2016.02.008.

Solomina, O.N., Bradley, R.S., Jomelli, V., Geirsdottir, A., Kaufman, D.S., Koch, J., McKay, N.P., Masiokas, M., Miller, G., Nesje, A., Nicolussi, K., Owen, L.A., Putnam, A.E., Wanner, H., Wiles, G., Yang, B., 2016b. Glacier fluctuations during the past 2000 years. Quat. Sci. Rev. 149, 61–90. https://doi.org/10.1016/j.quascirev.2016.04.008.

Sommer, C., Malz, P., Seehaus, T.C., Lippl, S., Zemp, M., Braun, M.H., 2020. Rapid glacier retreat and downwasting throughout the European Alps in the early 21st century. Nat. Commun. 11, 3209. https://doi.org/10.1038/s41467-020-16818-0.

Steger, C.R., Reijmer, C.H., van den Broeke, M.R., Wever, N., Forster, R.R., Koenig, L.S., Kuipers Munneke, P., Lehning, M., Lhermitte, S., Ligtenberg, S.R.M., Miège, C., Noël, B.P.Y., 2017. Firn meltwater retention on the Greenland ice sheet: a model comparison. Front. Earth Sci. 5. https://doi.org/10.3389/feart.2017.00003.

Stokes, C.R., Gurney, S.D., Shahgedanova, M., Popovnin, V., 2006. Late-20th-century changes in glacier extent in the Caucasus Mountains, Russia/Georgia. J. Glaciol. 52 (176), 99–109. https://doi.org/10.3189/172756506781828827.

Stokes, C.R., Shahgedanova, M., Evans, I.S., Popovnin, V.V., 2013. Accelerated loss of alpine glaciers in the Kodar Mountains, south-eastern Siberia. Glob. Planet. Change. 101https://doi.org/10.1016/j.gloplacha.2012.12.010.

The IMBIE Team, 2020. Mass balance of the Greenland ice sheet from 1992 to 2018. Nature 579, 233–239. https://doi.org/10.1038/s41586-019-1855-2.

The IMBIE Team, 2018. Mass balance of the Antarctic ice sheet from 1992 to 2017. Nature 558, 219–222. https://doi.org/10.1038/s41586-018-0179-y.

Thibert, E., Eckert, N., Vincent, C., 2013. Climatic drivers of seasonal glacier mass balances: an analysis of 6 decades at glacier de Sarennes (French Alps). Cryosphere 7, 47–66. https://doi.org/10.5194/tc-7-47-2013.

Thomas, E.R., Melchior Van Wessem, J., Roberts, J., Isaksson, E., Schlosser, E., Fudge, T.J., Vallelonga, P., Medley, B., Lenaerts, J., Bertler, N., Van Den Broeke, M.R., Dixon, D.A., Frezzotti, M., Stenni, B., Curran, M., Ekaykin, A.A., 2017. Regional Antarctic snow accumulation over the past 1000 years. Clim. Past 13, 1491–1513. https://doi.org/10.5194/cp-13-1491-2017.

Treydte, K.S., Schleser, G.H., Helle, G., Frank, D.C., Winiger, M., Haug, G.H., Esper, J., 2006. The twentieth century was the wettest period in northern Pakistan over the past millennium. Nature 440, 1179–1182. https://doi.org/10.1038/nature04743.

Trusel, L.D., Das, S.B., Osman, M.B., Evans, M.J., Smith, B.E., Fettweis, X., McConnell, J.R., Noël, B.P.Y., van den Broeke, M.R., 2018. Nonlinear rise in Greenland runoff in response to post-industrial Arctic warming. Nature 564, 104–108. https://doi.org/10.1038/s41586-018-0752-4.

van den Broeke, M., Box, J., Fettweis, X., Hanna, E., Noël, B., Tedesco, M., van As, D., van de Berg, W.J., van Kampenhout, L., 2017. Greenland ice sheet surface mass loss: recent developments in observation and modeling. Curr. Clim. Chang. Rep. 3, 345–356. https://doi.org/10.1007/s40641-017-0084-8.

van den Broeke, M.R., Enderlin, E.M., Howat, I.M., Kuipers Munneke, P., Noël, B.P.Y., Jan Van De Berg, W., Van Meijgaard, E., Wouters, B., 2016. On the recent contribution of the Greenland ice sheet to sea level change. Cryosphere 10, 1933–1946. https://doi.org/10.5194/tc-10-1933-2016.

Velicogna, I., 2009. Increasing rates of ice mass loss from the Greenland and Antarctic ice sheets revealed by GRACE. Geophys. Res. Lett. 36, 2–5. https://doi.org/10.1029/2009GL040222.

Vinther, B.M., Buchardt, S.L., Clausen, H.B., Dahl-Jensen, D., Johnsen, S.J., Fisher, D.A., Koerner, R.M., Raynaud, D., Lipenkov, V., Andersen, K.K., Blunier, T., Rasmussen, S.O., Steffensen, J.P., Svensson, A.M., 2009. Holocene thinning of the Greenland ice sheet. Nature 461, 385–388. https://doi.org/10.1038/nature08355.

Viviroli, D., Kummu, M., Meybeck, M., Kallio, M., Wada, Y., 2020. Increasing dependence of lowland populations on mountain water resources. Nat. Sustain. 3, 917–928. https://doi.org/10.1038/s41893-020-0559-9.

Viviroli, D., Weingartner, R., 2004. The hydrological significance of mountains: from regional to global scale. Hydrol. Earth Syst. Sci. 8, 1017–1030. https://doi.org/10.5194/hess-8-1017-2004.

Vuille, M., Francou, B., Wagnon, P., Juen, I., Kaser, G., Mark, B.G., Bradley, R.S., 2008. Climate change and tropical Andean glaciers: past, present and future. Earth Sci. Rev. 89, 79–96. https://doi.org/10.1016/j.earscirev.2008.04.002.

Wahr, J., Swenson, S., Zlotnicki, V., Velicogna, I., May, A., 2004. Time-variable gravity from GRACE: first results. Geophys. Res. Lett. 31, 20–23. https://doi.org/10.1029/2004GL019779.

Winkler, S., Chinn, T., Gärtner-Roer, I., Nussbaumer, S.U., Zemp, M., Zumbühl, H.J., 2010. An introduction to mountain glaciers as climate indicators with spatial and temporal diversity. Erdkunde 64, 97–118. https://doi.org/10.3112/erdkunde.2010.02.01.

Wouters, B., Bamber, J.L., van den Broeke, M.R., Lenaerts, J.T.M., Sasgen, I., 2013. Limits in detecting acceleration of ice sheet mass loss due to climate variability. Nat. Geosci. 6, 613–616. https://doi.org/10.1038/ngeo1874.

Wouters, B., Gardner, A.S., Moholdt, G., 2019. Global glacier mass loss during the GRACE satellite Mission (2002-2016). Front. Earth Sci. 7, 1–11. https://doi.org/10.3389/feart.2019.00096.

Wouters, B., Martin-Espanol, A., Helm, V., Flament, T., van Wessem, J.M., Ligtenberg, S.R.M., van den Broeke, M.R., Bamber, J.L., 2015. Dynamic thinning of glaciers on the southern Antarctic peninsula. Science 348, 899–903. https://doi.org/10.1126/science.aaa5727.

Yang, R., Hock, R., Kang, S., Shangguan, D., Guo, W., 2020. Glacier mass and area changes on the Kenai peninsula, Alaska, 1986–2016. J. Glaciol. 66 (258), 603–607. https://doi.org/10.1017/jog.2020.32.

Zemp, M., Frey, H., Gärtner-Roer, I., Nussbaumer, S.U., Hoelzle, M., Paul, F., Haeberli, W., Denzinger, F., Ahlstrøm, A.P., Anderson, B., Bajracharya, S., Baroni, C., Braun, L.N., Cáceres, B.E., Casassa, G., Cobos, G., Dávila, L.R., Delgado Granados, H., Demuth, M.N., Espizua, L., Fischer, A., Fujita, K., Gadek, B., Ghazanfar, A., Ove Hagen, J., Holmlund, P., Karimi, N., Li, Z., Pelto, M., Pitte, P., Popovnin, V.V., Portocarrero, C.A., Prinz, R., Sangewar, C.V., Severskiy, I., Sigurđsson, O., Soruco, A., Usubaliev, R., Vincent, C., 2015. Historically unprecedented global glacier decline in the early 21st century. J. Glaciol. 61 (228), 745–762. https://doi.org/10.3189/2015JoG15J017.

Zemp, M., Hoelzle, M., Haeberli, W., 2009. Six decades of glacier mass-balance observations: a review of the worldwide monitoring network. Ann. Glaciol. 50, 101–111. https://doi.org/10.3189/172756409787769591.

Zemp, M., Huss, M., Thibert, E., Eckert, N., McNabb, R., Huber, J., Barandun, M., Machguth, H., Nussbaumer, S.U., Gärtner-Roer, I., Thomson, L., Paul, F., Maussion, F., Kutuzov, S., Cogley, J.G., 2019. Global glacier mass changes and their contributions to sea-level rise from 1961 to 2016. Nature 568, 382–386. https://doi.org/10.1038/s41586-019-1071-0.